



# Design, synthesis, and biological evaluation of novel bifunctional thyrointegrin antagonists for neuroblastoma

Ozlem Ozen Karakus, Kavitha Godugu, Kazutoshi Fujioka, Shaker A. Mousa<sup>\*</sup>

Pharmaceutical Research Institute, Albany College of Pharmacy and Health Sciences, Rensselaer, NY 12144, United States

## ARTICLE INFO

### Keywords:

Dual targeting  
Drug-drug Conjugate  
Integrin  $\alpha\beta 3$   
Norepinephrine transporter (NET)  
Neuroblastoma  
Thyrointegrin antagonist

## ABSTRACT

Receptor-mediated cancer therapy has received much attention in the last few decades. Neuroblastoma and other cancers of the sympathetic nervous system highly express norepinephrine transporter (NET) and cell plasma membrane integrin  $\alpha\beta 3$ . Dual targeting of the NET and integrin  $\alpha\beta 3$  receptors using a Drug-Drug Conjugate (DDC) might provide effective treatment strategy in the fight against neuroblastoma and other neuroendocrine tumors. In this work, we synthesized three dual-targeting BG-P<sub>400</sub>-TAT derivatives, di-BG-P<sub>400</sub>-TAT, dM-BG-P<sub>400</sub>-TAT, and BG-P<sub>400</sub>-PAT containing di-iodobenzene, di-methoxybenzene, and piperazine groups, respectively. These derivatives utilize to norepinephrine transporter (NET) and the integrin  $\alpha\beta 3$  receptor to simultaneously modulate both targets based on evaluation in a neuroblastoma animal model using the neuroblastoma SK-N-F1 cell line. Among the three synthesized agents, the piperazine substituted BG-P<sub>400</sub>-PAT exhibited potent integrin  $\alpha\beta 3$  antagonism and reduced neuroblastoma tumor growth and cancer cell viability by >90%. In conclusion, BG-P<sub>400</sub>-PAT and derivatives represent a potential therapeutic approach in the management of neuroblastoma.

## 1. Introduction

Neuroblastoma is the most common extracranial solid tumor in babies and the third-most common cancer in children after leukemia and brain cancer<sup>1</sup>. It most frequently (65% of cases) starts from the abdomen and arises in the medulla of the adrenal gland. However, it can develop in the chest (20%), pelvis (3%), or neck (2%)<sup>2,3</sup>. Several chemotherapeutic agents are used to treat neuroblastoma such as cisplatin, vincristine, rapamycin, carboplatin, etoposide, cyclophosphamide and 13-*cis*-retinoic acid<sup>4,5</sup>. However, drug resistance and toxicity often cause treatment failure<sup>6-8</sup>. Therefore, the development of new anticancer strategies is crucial to overcome drug resistance and safety issues for better management of neuroblastoma.

Neuroblastoma cells are derived from neural crest and they show high norepinephrine transporter (NET) expression, which is a transmembrane protein encoded by the *SLC6A2* gene. NET actively transports norepinephrine, a catecholamine hormone made by the adrenal glands, from the synapse into presynaptic neurons. Norepinephrine structural analogues of neuro-adrenergic blocking agents guanethidine and bretylium compete with norepinephrine for uptake and storage by neuroendocrine cells. Benzylguanidine (BG), is known as a metabolically

stable norepinephrine structural analogue<sup>9,10</sup>, which can be taken up by NET, and accumulate in the cytoplasm and mitochondria<sup>11,12</sup>. Because BG competes with norepinephrine for uptake and storage by neuroendocrine cells, it can be used as both a targeting agent and as treatment for neuroblastomas<sup>12,13</sup>.

Another family of proteins, the integrins, regulate the growth, invasion and metastatic process of neuroblastomas and other tumors. Integrins are a family of heterodimeric cell surface receptors that consist of 24 subunits designated  $\alpha$  and  $\beta$ . Integrins can mediate cell adhesion, proliferation, and survival by interacting with proteins of the extracellular matrix<sup>14</sup>. Abnormal regulation of integrins on cancer cells and surrounding tissues compared to normal cells plays a key role in tumor progression and pathological angiogenesis—angiogenesis is an essential process for oxygen and nutrient supply for tumor growth<sup>15</sup>. Integrin  $\alpha\beta 3$ , a plasma membrane integrin that has a receptor for thyroid hormones, is upregulated in both tumor cells and angiogenic endothelial cells, thus blocking upregulation of integrin  $\alpha\beta 3$  via integrin antagonists can be an approach to combat tumor progression and metastasis for neuroblastomas<sup>16,17</sup>.

The most common integrin recognition motif, tripeptide Arg-Gly-Asp (RGD), is responsible for cell adhesion to the extracellular matrix protein

<sup>\*</sup> Corresponding author at: The Pharmaceutical Research Institute, Albany College of Pharmacy and Health Sciences, 1 Discovery Drive (Room 238), Rensselaer, NY 12144, USA.

E-mail address: [shaker.mousa@acphs.edu](mailto:shaker.mousa@acphs.edu) (S.A. Mousa).

<https://doi.org/10.1016/j.bmc.2021.116250>

Received 26 March 2021; Received in revised form 10 May 2021; Accepted 28 May 2021

Available online 6 June 2021

0968-0896/© 2021 Elsevier Ltd. All rights reserved.

(ECM). Integrin receptors recognize the RGD sequence and RGD can bind to many types of integrins. Therefore, RGD-containing peptides have been taken advantage of to design effective integrin  $\alpha\beta3$  antagonists<sup>18–20</sup>. Recent studies stated that in addition to integrin antagonists, thyroid hormone antagonists can also regulate angiogenesis<sup>21–23</sup>. The effects of thyroid hormone analogs on the integrin  $\alpha\beta3$  thyroid hormone receptor and membrane  $\text{Na}^+/\text{H}^+$  anti-porter ion pumps were also investigated and a complex relationship was found between thyroid hormone and angiogenesis<sup>24</sup>. The thyroid hormone agonist analogs have been shown to induce angiogenesis, while the metabolic degradation product of thyroid hormone, tetraiodothyroacetic acid (tetrac), inhibits angiogenesis<sup>25,26</sup>. Tetrac is a deaminated derivative of thyroid hormone L-thyroxine ( $\text{T}_4$ ) and functions as a thyroid hormone antagonist by blocking the actions of triiodothyronine ( $\text{T}_3$ ) and  $\text{T}_4$  at the thyroid hormone receptor site on integrin  $\alpha\beta3$ <sup>25,27,28</sup>. Thus, we called this specific type of ligand that blocks both thyroid hormones and integrin  $\alpha\beta3$  receptor sites a “thyrointegrin  $\alpha\beta3$ ” antagonist<sup>29</sup>.

In the past decade, our group developed a series of high affinity thyrointegrin  $\alpha\beta3$  antagonists<sup>30–32</sup>. One of these studies was the design of a polymeric antagonist containing two tetrac groups with a triazole ring (triazole tetrac, TAT), called P-bi-TAT, which was then investigated for its anticancer activities in glioblastoma tumors<sup>33</sup>. In another study, we designed and synthesized a dual Drug-Drug Conjugate (DDC) targeting ligand and named it BG-P<sub>400</sub>-TAT; it contains polyethylene glycol (PEG) with about 400 g/mol molar mass and we investigated its anticancer activity for neuroblastoma<sup>34,35</sup>. In that case, we used BG for NET targeting and triazole tetrac (TAT) for integrin  $\alpha\beta3$  targeting. Based on the promising results from that study, for enhanced  $\alpha\beta3$  integrin binding affinity of BG-P<sub>400</sub>-TAT derivatives to neuroblastoma cells. Thus, we chose two substituents, iodo and methoxy, for the BG aromatic unit to change the hydrophilicity of the aromatic ring for interaction with target protein. We also examined the effect of a basic linker, piperazine by replacing the triazole linker to form piperazine tetrac

(PAT). So, here we synthesized three different derivatives of BG-P-TAT (Fig. 1), di-BG-P<sub>400</sub>-TAT (7a), dM-BG-P<sub>400</sub>-TAT (7b), and BG-P<sub>400</sub>-PAT (15) and evaluated their  $\alpha\beta3$  binding affinity and anticancer efficacy in neuroblastoma xenograft mice model.

We are the first group to develop thyrointegrin  $\alpha\beta3$  antagonist that contain tetrac, a thyromimetic that is very effective against various cancers but with limited efficacy against neuroendocrine cancers because of its limited access and transport into neuroendocrine tumors such as neuroblastoma despite their  $\alpha\beta3$  high affinity. However, optimal anticancer efficacy was achieved upon conjugation of different thyrointegrin  $\alpha\beta3$  antagonists via polyethylene glycol to MIBG derivative (Benzyl Guanidine), a known NET transporter utilized for targeted radiation delivery and imaging of neuroendocrine cancers.

## 2. Results and discussion

### 2.1. Design and strategy

We have elsewhere demonstrated that BG-P<sub>400</sub>-TAT exhibited 6-fold higher binding affinity towards integrin  $\alpha\beta3$  with lower 50% inhibitory concentration  $\text{IC}_{50} = 10.32$  nM versus tetrac<sup>35</sup>. That study also showed that para substitution of BG did not change its therapeutic activity on neuroblastoma tumor cells.

Here, we examined the effect of meta substitution on BG for targeting NET transporter. Iodo and methoxy groups were chosen as meta substituents on the BG aromatic ring. The iodo group withdraws electrons through an inductive effect from the aromatic ring, and methoxy donates its lone pairs on the oxygen atom through a resonance effect to the aromatic ring. The binding sites of both targeted proteins, NET, and integrin  $\alpha\beta3$ , consist of several hydrophobic residues. Increased hydrophilicity of the BG-P<sub>400</sub>-TAT with iodo groups may enhance its binding affinity via van der Waals interactions. We also tried methoxy group as substituent to make a more electron rich aromatic ring than the non-substituted BG, and this substitution not only increased  $\pi$ -cation interactions but also increased binding affinity of the compound towards the targeted proteins. Other polar interactions such as dipole–dipole and hydrogen bonding also play a role in increasing binding affinity<sup>9</sup>. Therefore, we replaced the neutral triazole linker with basic piperazine for attaching tetrac and PEG units to study the effect of polar interactions on the binding. Br and N<sub>3</sub> functionalized PEG6 and PEG7 used for conjugation in this report.

### 2.2. Chemistry

The synthesis of di-BG-P<sub>400</sub>-TAT (7a) and dM-BG-P<sub>400</sub>-TAT (7b) was accomplished as described in Scheme 1. Amine groups of iodo and methoxy substituted 4-hydroxy benzyl amine were protected with *tert*-butyl di-carbonate. Compounds 2a and 2b were characterized with <sup>1</sup>H NMR (Figs. S1 and S3). The peak observed at 1.49 ppm was assigned to *tert*-butyloxycarbonyl (Boc) protons. In the next reaction, compounds 2a and 2b were reacted with commercially available Br-PEG6-N<sub>3</sub> in the presence of K<sub>2</sub>CO<sub>3</sub> and ACN under reflux conditions to get compound 3a and 3b with 90% and 85% yields, respectively. The <sup>1</sup>H NMR spectra of compounds 3a and 3b (Figs. S5 and S7) exhibited peaks of PEG protons between 3.40 and 3.97 ppm. Then, we deprotected amino groups in 4 N HCl (in dioxane) and confirmed the product by disappearance of Boc-proton signals at 1.48 and 1.49 ppm in the <sup>1</sup>H NMR spectra of 4a and 4b (Figs. S9 and S11). In the next step, N,N'-di-Boc-1H-pyrazole-1-carboxamide was reacted with compounds 4a and 4b to acquire Boc-protected guanidine compounds 5a and 5b. The <sup>1</sup>H NMR spectra of compounds 5a and 5b (Figs. S13 and S15) clearly showed peaks at 1.49–1.52 and 1.50–1.52 ppm, respectively, which can be assigned to two separate Boc groups' protons.

Then, azide-containing compounds 5a and 5b were conjugated with propargylated tetrac, (PGT)<sup>36</sup>, which is terminal alkyne-containing tetrac, in a click reaction by forming a triazole ring to get compounds 6a

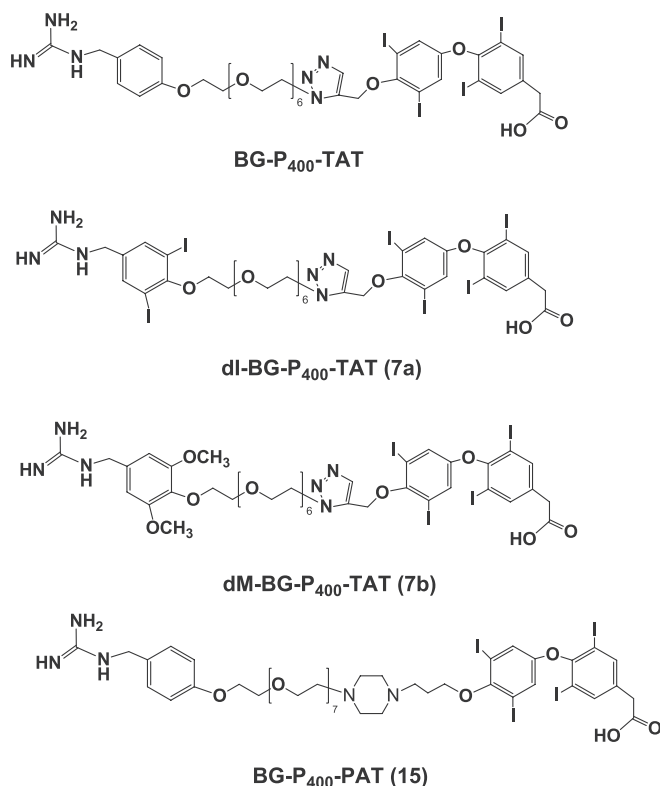
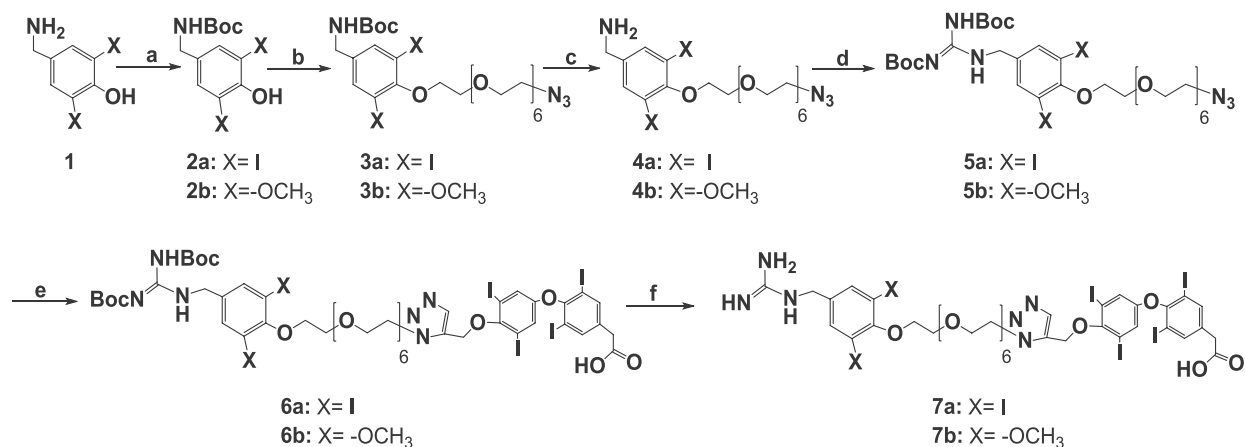


Fig. 1. Chemical structures of BG-P<sub>400</sub>-TAT, di-BG-P<sub>400</sub>-TAT, dM-BG-P<sub>400</sub>-TAT, and BG-P<sub>400</sub>-PAT (BG, benzyl guanidine; TAT, triazole tetrac; PAT, piperazine tetrac).



**Scheme 1.** Synthesis diagram of compounds **7a** and **7b**. (a)  $\text{Boc}_2\text{O}$ , 6 h; (b)  $\text{K}_2\text{CO}_3$ , ACN, Br-PEG6- $\text{N}_3$ , reflux, 24 h; (c) HCl (4 N in dioxane), rt, 4 h; (d) DCM, TEA,  $N,N'$ -di-Boc-1H-pyrazole-1-carboxamide, rt, 12 h; (e) PGT, THF:water 4:1,  $\text{CuSO}_4$ , Na Ascorbate, rt, 24 h; (f) HCl (4 N in dioxane), rt, 24 h.

and **6b**.  $\text{CuSO}_4/\text{Na Ascorbate}$  (0.3 eq:0.6 eq) in THF :water (4:1) was used to generate  $\text{Cu}^+$  in situ at room temperature. The characteristic singlet peak of triazole ring protons appeared at 8.59 and 8.60 ppm in the  $^1\text{H}$  NMR spectra of compounds **6a** and **6b**, respectively. (Figs. S17, S19). Lastly, protecting Boc groups were removed in 4 N HCl (in dioxane), and the resulting product was purified with reverse phase column chromatography with MeOH:water (70:30) to get compounds **7a** and **7b**. The  $^1\text{H}$  NMR (Figs. S21, S23),  $^{13}\text{C}$  NMR (Figs. S22, S24), and mass spectra (Figs. S29, S31) of compounds **7a** and **7b** confirmed their structure.

The synthesis of BG-P400-PAT **15** was accomplished as described in Scheme 2. First, the amino group of 4-hydroxybenzyl amine **8** was protected with Boc group. Then, Br-PEG7-OH was reacted with the phenolic OH group of **9** in the presence of  $\text{K}_2\text{CO}_3$  and ACN at reflux temperature to get **10**, and it was characterized with  $^1\text{H}$  NMR by observing PEG proton peaks at 3.6–3.8 ppm (Fig. S34).

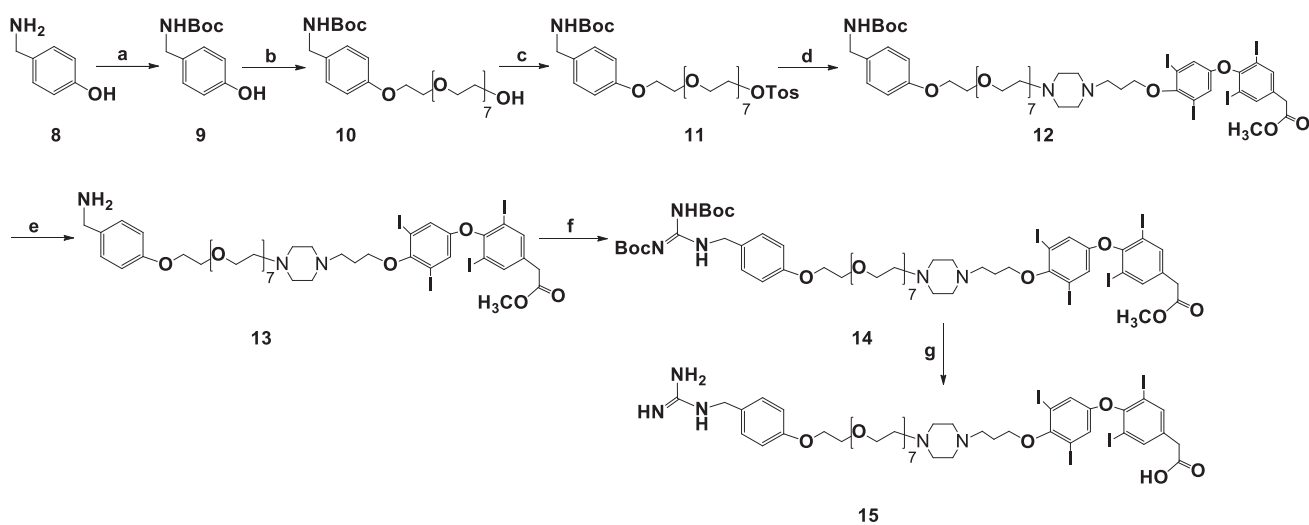
A different method was used to introduce a tetrac unit on the PEG (Scheme 3). First, carboxylic acid group of tetrac **16** was converted to methyl ester in MeOH and  $\text{SOCl}_2$  to get **17**. Then it was reacted with *tert*-butyl 4-(3-(methanesulfonyloxy)propyl)piperazine-1-carboxylate hydrochloride **18** and  $\text{Cs}_2\text{CO}_3$  as a base in ACN, followed by treatment with HCl (4 N in dioxane) solution to deprotect the Boc group. The structure of resulting compound **19** was characterized with  $^1\text{H}$  NMR (Fig. S38).

Aromatic protons of tetrac were observed at 7.32 and 8.04 ppm and piperazine protons were observed at 2.77 and 2.94 ppm.

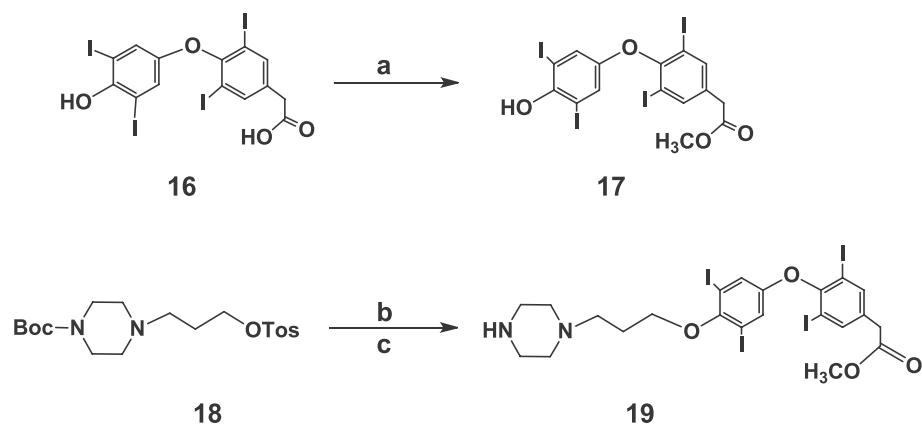
Compound **19** was introduced (Scheme 2) to a PEG unit after the tosylation reaction of PEG-OH **10** in the presence of  $\text{K}_2\text{CO}_3$  and ACN to give compound **12**. The  $^1\text{H}$  NMR spectrum of **12** (Fig. S40) confirmed the structure by observing tetrac and *N*-Boc benzylamine aromatic proton peaks at 7.18–7.79 and 6.88–7.20, respectively. After *N*-Boc deprotection of compound **12**, free amine of **13** was used with  $N,N'$ -di-Boc-1H-pyrazole-1-carboxamide in DCM and TEA as a base to introduce Boc-protected guanidine group and afforded compound **14**. Finally, methyl ester and Boc protection groups were hydrolyzed with conc. HCl in dioxane :water to give desired compound **15**.  $^1\text{H}$  NMR (Fig. S46) and the mass spectrum (Fig. S53) of **15** confirmed its structure. Purities of final synthesized products **7a**, **7b**, and **15** were confirmed to be > 95% by HPLC (Figs. S55–S57).

### 2.3. Integrin binding affinity

DDC Compounds di-BG-P400-TAT (**7a**), dM-BG-P400-TAT (**7b**), and BG-P400-PAT (**15**) showed relatively higher binding affinity towards purified integrin  $\alpha\text{v}\beta_3$  receptor with lower  $\text{IC}_{50}$  values 1.1 nM, 0.5 nM, and 0.3 nM, respectively, compared to 10.3 nM for BG-P400-TAT (Fig. 2) by introducing *m*-substituents on the BG ring (**7a** and **7b**). This is most



**Scheme 2.** Synthesis diagram of compound **15**. (a)  $\text{Boc}_2\text{O}$ , 6 h; (b)  $\text{K}_2\text{CO}_3$ , ACN, Br-PEG7-OH reflux, 24 h; (c) Tos-Cl, DCM, TEA, 0 °C-rt, 2 h; (d) compound **19** (see Scheme 3), ACN,  $\text{K}_2\text{CO}_3$  60 °C, 18 h; (e) HCl (4 N in dioxane), rt, 4 h; (f) DCM, TEA,  $N,N'$ -di-Boc-1H-pyrazole-1-carboxamide, rt, 12 h; (g) dioxane:water, conc. HCl, rt, 24 h.



**Scheme 3.** Synthesis diagram of compound 19. (a)  $\text{SOCl}_2$ , MeOH; (b) 17, ACN,  $\text{Cs}_2\text{CO}_3$ , 60 °C, 18 h; (c) 4 N HCl in dioxane, 2 h.

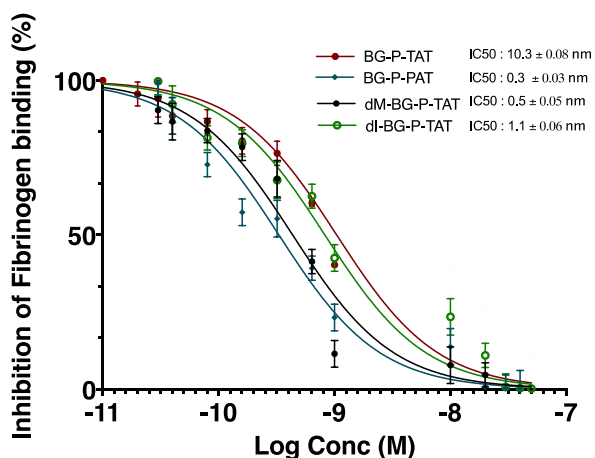


**Fig. 2.** Binding affinities of dI-BG-P<sub>400</sub>-TAT, dM-BG-P<sub>400</sub>-TAT, and BG-P<sub>400</sub>-PAT compared to BG-P<sub>400</sub>-TAT towards purified integrin  $\alpha\text{v}\beta 3$  receptor.

likely due to increased van der Waals and  $\pi$ -cation interactions between receptor and ligand with newly added iodine and methoxy groups. On the other hand, keeping the BG ring and replacing the triazole linker with piperazine increased the binding affinity towards integrin  $\alpha\text{v}\beta 3$  receptor. This phenomenon can be explained with various factors such as newly formed hydrogen bonds between basic piperazine and integrin  $\alpha\text{v}\beta 3$  receptor. Also, linker chain length might affect accommodation of the molecule in the  $\alpha\text{v}\beta 3$  binding pocket side because BG-P-PAT (15), with a slightly longer linker chain, has a 30-fold increase in binding affinity relative to BG-P-TAT.

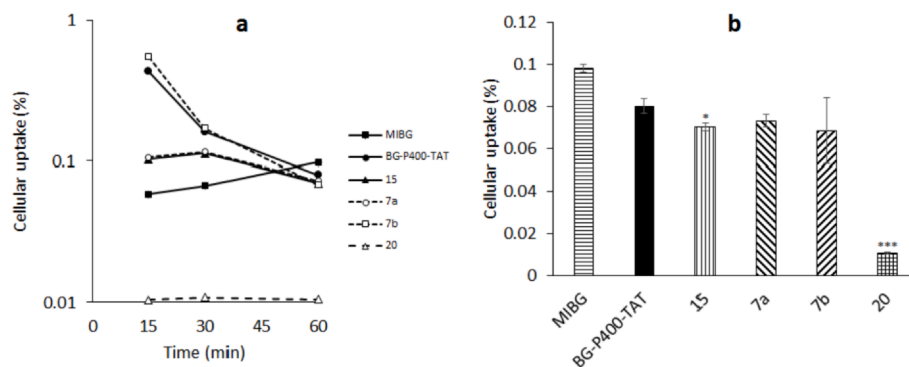


**Fig. 3.** (a) The cellular uptake of MIPG, BG-P<sub>400</sub>-TAT, BG-P<sub>400</sub>-PAT (15), dI-BG-P<sub>400</sub>-TAT (7a), dM-BG-P<sub>400</sub>-TAT in neuroblastoma cells (7b) and 20 in SK-N-F1 neuroblastoma cells incubated at a concentration of 10  $\mu\text{M}$  for 15, 30 and 60 min. (b) The uptake of MIPG, BG-P<sub>400</sub>-TAT and derivatives in SK-N-F1 neuroblastoma cells (~1M), concentration of 10  $\mu\text{M}$  at 60 min. \*: P-value < 0.05 compared with BG-P<sub>400</sub>-TAT. \*\*\*: P-value < 0.001 compared with BG-P<sub>400</sub>-TAT.

#### 2.4. *In vitro* cellular uptake

MIBG, BG-P<sub>400</sub>-TAT<sup>35</sup>, dI-BG-P<sub>400</sub>-TAT (7a), dM-BG-P<sub>400</sub>-TAT (7b), BG-P<sub>400</sub>-PAT (15) and at *N*-Boc-Benzylamine-P<sub>400</sub>-TAT (20) 1  $\mu\text{M}$  were incubated with SK-N-F1 neuroblastoma cells (~1M) for 15, 30, and 60 min (Fig. 3). 20 was included in this test as a negative control since it has a moiety of integrin  $\alpha\text{v}\beta 3$  binding (TAT) but lacks a moiety of NET binding pocket. Substrates in cells were extracted and quantified with LC-MS/MS. The uptake of MIBG was the highest at 60 min, followed by BG-P<sub>400</sub>-TAT, 7a, 7b, and 20 (Fig. 3a). The uptake of BG-P<sub>400</sub>-TAT and derivatives were comparable to each other and more than 20 (Fig. 3b). The increased uptake of BG-P<sub>400</sub>-TAT and derivatives compared with 20 suggest that they are actively transported with facilitation of NET.

#### 2.5. Molecular docking

Molecular docking studies were carried out with 7a, 7b, and 15 to understand the mode of binding and type of interaction with the active site of integrin  $\alpha\text{v}\beta 3$  (PDB:1L5G) by using auto dock tools (Figs. S58, S59). The molecular docking results show a bent structure of the molecules at the binding site. The interaction and docking analysis revealed that 15 has the best interaction rate with high binding energy  $-14.4$  kcal/mol and forms 9 hydrogen bonds with integrin  $\beta 3$  subunit (Fig. 4). 7a and 7b had binding energies of  $-6.1$  kcal/mol and  $-7.8$  kcal/mol, respectively, and 7a formed 6 hydrogen bonds (1 with  $\alpha\text{v}$  domain and 5 with  $\beta 3$  domain) and 7b formed 6 hydrogen bonds (1 with  $\alpha\text{v}$  domain, 4 with  $\beta 3$  domain and 1 with Mn atom). Energy values for 7a, 7b, and 15 with binding energies and residues involved in interactions are listed in Table 1. The 30-fold higher  $\alpha\text{v}\beta 3$  binding affinity of 15 versus the close analog BG-P<sub>400</sub>-TAT may be due to the additional hydrogen bonds of the

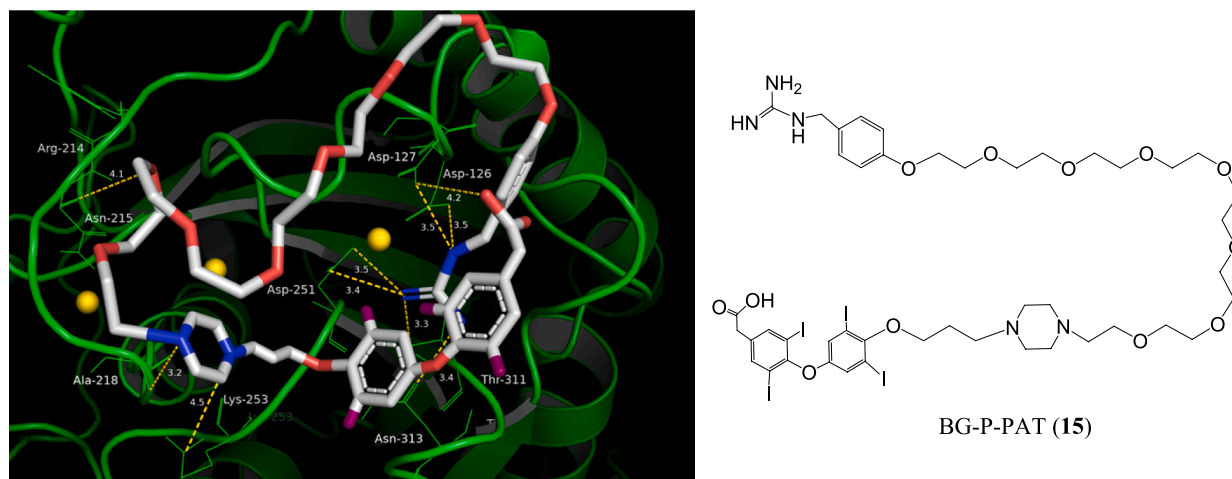


**Fig. 4.** Binding mode of BG-P-PAT (**15**) with the crystal structure of integrin  $\alpha\beta 3$  (left) (PDB ID 1L5G) and structure of compound **15** (right). Dashed yellow lines show hydrogen bonds, integrin subunit  $\beta 3$  is shown in green.

**Table 1**  
Binding energies of the compounds with integrin  $\alpha\beta 3$ .

Compound	Docking Score (kcal/mol)	Interacting Residues		Bond Distance (Å)
		A-chain ( $\alpha$ -subunit)	B-chain ( $\beta$ -subunit)	
dI-BG-P-TAT ( <b>7a</b> )	-6.1	Tyr 178	Tyr-166	2.9
			Arg 214	3
			Ser 334	2.8
			Ser 337	2.5
			Lys 125	3.7
dM-BG-P-TAT ( <b>7b</b> )	-7.8	Tyr 178	Arg 216	3.2
			Ser 334	2.2, 2.2, 4.5
			Mn	2.4
				4.8
BG-P-PAT ( <b>15</b> )	-14.4		Asp 126	3.5
			Asp 127	3.5, 4.2
			Arg 214	4.1
			Asn 215	3.8
			Ala 218	3.2
			Asp 251	3.5, 3.4
			Lys 253	4.5
			Thr 311	3.4
			Asn 313	3.3

BG portion of **15** in with Asp-127 and Asp-126. This may be a result of the longer linker chain in BG-P<sub>400</sub>-PAT, allowing the BG portion easier access to this domain than the BG in BG-P<sub>400</sub>-TAT. Additional hydrogen bonding of the piperazine nitrogen may also be responsible for some of the increased  $\alpha\beta 3$  binding affinity of BG-P<sub>400</sub>-PAT.

## 2.6. *In vivo* anticancer efficacy

dI-BG-P<sub>400</sub>-TAT (**7a**), dM-BG-P<sub>400</sub>-TAT (**7b**), and BG-P<sub>400</sub>-PAT (**15**) at 3 mg kg<sup>-1</sup> were administered subcutaneously (s.c.) daily for 20 days to nude mice implanted with the SK-N-F1 neuroblastoma cell line for comparative anticancer activities. The tumor volumes significantly decreased compared to control (Fig. 5A). Compound **15** treatment resulted in significant decrease in tumor weight by 90%, and compounds **7b** and **7a** resulted in 86% and 67% decreases in tumor weight, respectively (Fig. 5B). For compound **7a**, the treatment was discontinued, and animals were terminated for after 7 days due to skin irritation of the mice.

## 2.7. Histopathology

To compare the histopathological changes in tumors of untreated and treated groups, tumors were harvested, fixed, and stained with hematoxylin and eosin (H&E). Necrosis at low magnification of tumors

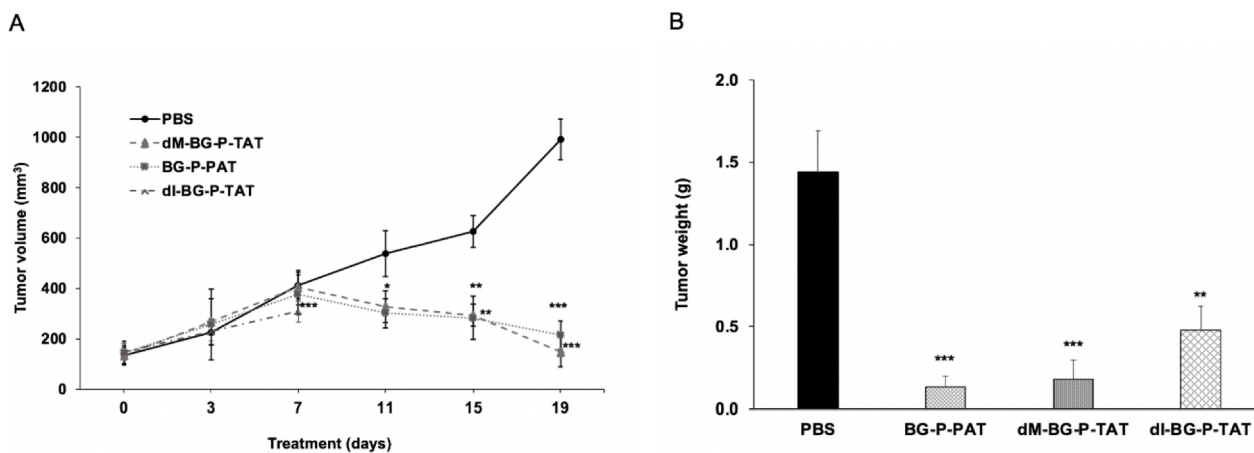


**Fig. 5.** Comparative (A) tumor volumes and (B) tumor weights of dI-BG-P<sub>400</sub>-TAT, dM-BG-P<sub>400</sub>-TAT, and BG-P<sub>400</sub>-PAT at treatment dose of 3 mg kg<sup>-1</sup> body weight once a day subcutaneously for 20 days compared to vehicle control (PBS). The treatment with dI-BG-P<sub>400</sub>-TAT was discontinued after 7 days because of skin irritation at the injection site that caused pain and distress to those animals.

from animals treated with compounds **7a**, **7b**, and **15** versus control is seen clearly (Fig. 6). The staining showed large areas of necrosis, fibrosis, and cell debris with approximately 98% (**15**), 85% (**7b**), and 70% (**7a**). On the other hand, tumors from the untreated group had mostly viable tumor cells. At higher magnification (40 $\times$ ) of BG-P<sub>400</sub>-PAT (**15**), there were large areas of necrosis replaced with normal tissue. It is important to note that compound **7a** was administered for only 7 days versus 20 days for the other two compounds.

### 3. Conclusions

Recent data have highlighted that the BG-P<sub>400</sub>-TAT ligand dually targeting NET and integrin  $\alpha\beta 3$  shows more effective results in the treatment of neuroblastoma than administration of BG and TAT separately<sup>34,35</sup>. The current study developed the anticancer activities of dual targeting BG-P<sub>400</sub>-TAT derivatives for neuroblastoma. To enhance the potency towards target proteins NET and integrin  $\alpha\beta 3$  receptor, compound BG-P<sub>400</sub>-TAT<sup>35</sup> was modified by adding new substituents iodo (dI-BG-P<sub>400</sub>-TAT, **7a**) and methoxy (dM-BG-P<sub>400</sub>-TAT, **7b**) and replacing the triazole group with piperazine (BG-P<sub>400</sub>-PAT, **15**) as novel dual-targeting molecules. Compounds **7a** and **7b** demonstrated 67% and 86% tumor shrinkage, respectively, and compound **15** showed 90% shrinkage with maximal loss of cancer cell viability. These results for compounds **7b** and **15** are higher than those for previously synthesized BG-P<sub>400</sub>-TAT, which showed 80% tumor shrinkage.

In the *in vivo* studies of these derivatives (**7a**, **7b**, and **15**), results can be explained by their relatively higher binding affinity towards purified integrin  $\alpha\beta 3$  receptor with lower IC<sub>50</sub> values compared to parent compound BG-P<sub>400</sub>-TAT. Histopathology results of compounds **15** and **7b** showed 98% and 85% necrosis of cancer cells, respectively, and all these experimental results strongly support using these compounds for neuroblastoma therapy development, which has less than 40% overall patient survival. Hence, our dual NET thyrointegrin  $\alpha\beta 3$  antagonist BG-

P<sub>400</sub>-TAT derivatives (compounds **7b** and **15**) improve upon the original compound and may be promising new drug candidates for the treatment of neuroblastoma.

## 4. Methods

### 4.1. Chemicals and Analysis

4-Hydroxybenzylamine, di-*tert*-butyl dicarbonate, HCl (4 N in dioxane), N,N'-Di-Boc-1H-pyrazole-1-carboxamide, TEA, sodium ascorbate, and copper sulfate were purchased from Sigma-Aldrich. 4-Hydroxy-3,5-dimethoxy-benzylamine, 4-hydroxy-3,5-diiodo-benzylamine, and *tert*-butyl 4-(3-(methanesulfonyloxy)propyl)piperazine-1-carboxylate hydrochloride were purchased from Chem-Space, Labseeker, and Synthonyx, respectively. Br-PEG6-N<sub>3</sub> and OH-PEG7-N<sub>3</sub> were purchased from Broad Pharm. Propargylated tetrac (PGT) and methyl ester of tetrac were synthesized according to a published method<sup>36</sup>. All commercially available chemicals were used without further purification. All solvents were dried, and anhydrous solvents were obtained using activated molecular sieves (0.3 or 0.4 nm depending on solvent type). All reactions (if not specifically containing water as reactant, solvent, or co-solvent) were performed under N<sub>2</sub> atmosphere in oven-dried glassware. Chemical structures of all synthesized compounds were confirmed with <sup>1</sup>H NMR, <sup>13</sup>C NMR, and mass spectrometry. The NMR experiments were performed on a Bruker Advance II 800 MHz spectrometer at the Center for Biotechnology and Interdisciplinary Studies, Rensselaer Polytechnic Institute. Thin layer chromatography was performed on silica gel plates with fluorescent indicator. Visualization was accomplished with UV light (254 and/or 365 nm). High resolution mass spectral analysis was performed on either an Applied Biosystems API4000 LC/MS/MS or Advion Expression CMC<sup>L</sup>. Purity of all final compounds was  $\geq 95\%$  as determined by HPLC, Waters 2695 system equipped with a Pursuit XRs C18 column (150  $\times$  4.6 mm) with a flow rate of 1 mL/min using a

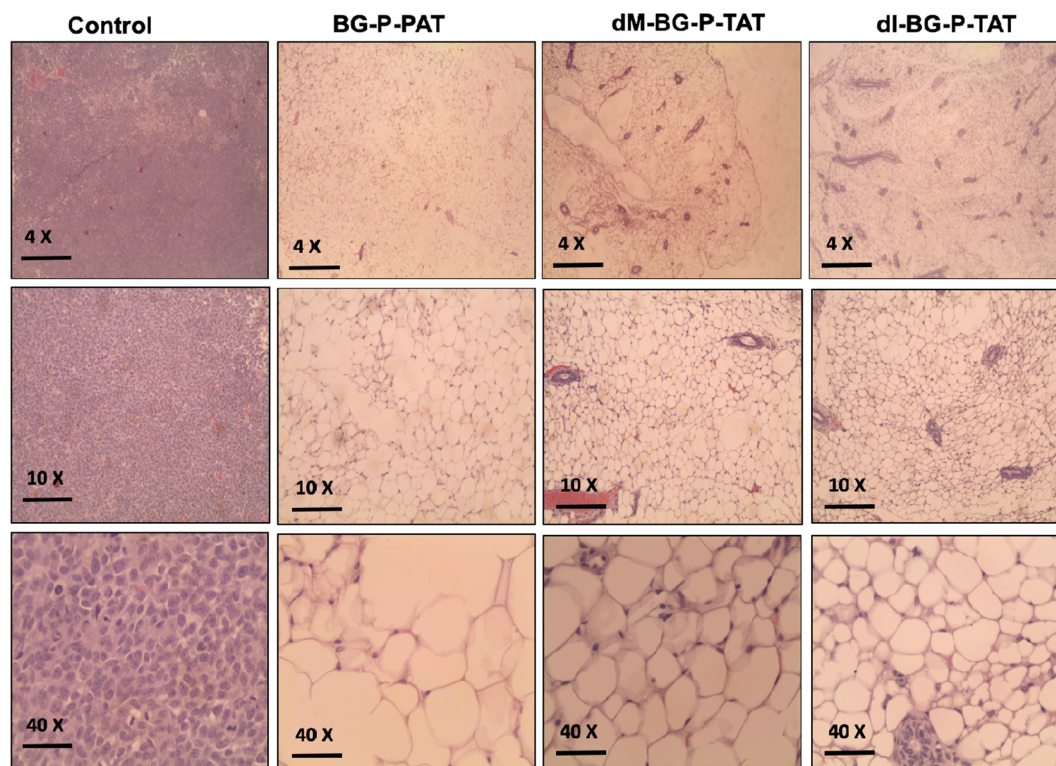


Fig. 6. Histology images showing the effect of compound **15** (BG-P-PAT), **7a** (dI-BG-P-TAT), and **7b** (dM-BG-P-TAT) after 20 days of daily treatment on SK-N-F1 neuroblastoma xenografts in mice at low power view (4X and 10X) and high-power view (40X) in histologic sections from untreated and treated animals. Sections from untreated animals showed complete infiltration with malignant cells (~100%) whereas sections from treated animals revealed complete necrosis, fibrosis, and inflammation.

gradient of MeOH and water (0.1% TFA) and UV detection at 227 and 254 nm.

#### 4.2. Synthesis of tert-butyl 4-hydroxy-3,5-diiodobenzylcarbamate (2a)

4-Hydroxy-3,5-diodo-benzylamine (750 mg, 1.8 mmol, 1 eq) was slowly added with stirring to a solution of di-tert-butyl dicarbonate (500 mg, 1.1 mmol, 1.1 eq) and NaHCO<sub>3</sub> (400 mg, 4.5 mmol, 2.5 eq) in MeOH:THF:water (1:2:2) mixture at room temperature. After the reaction mixture was stirred for 6 h, the solvent mixture was evaporated. The residue was dissolved in 50 mL DCM and washed with 1% HCl (25 mL) and brine (25 mL) and then dried (MgSO<sub>4</sub>) (Yield: 0.78 g, 90%). <sup>1</sup>H NMR (600 MHz, CDCl<sub>3</sub>): 1.49 (9H, s, *t*-butyl), 4.20 (2H, s, CH<sub>2</sub>), 4.87 (1H, s, OH), 5.77 (1H, s, NH), 7.62 (2H, s, ArH). <sup>13</sup>C NMR (150 MHz, CDCl<sub>3</sub>): 28.4, 42.6, 79.9, 82.2, 135.1, 137.6, 138.2, 152.3, 155.2. MS (ESI+): C<sub>12</sub>H<sub>15</sub>I<sub>2</sub>NO<sub>3</sub> · H<sup>+</sup> Calcd, 473.9 found: 473.9. Anal. Calcd. (%): C, 30.34; H, 3.18; N, 2.95. Found (%): C, 30.25; H, 3.25; N, 2.88.

#### 4.3. Synthesis of tert-butyl 4-hydroxy-3,5-dimethoxybenzylcarbamate (2b)

4-Hydroxy-3,5-dimethoxy-benzylamine (750 mg, 3.4 mmol, 1 eq) was slowly added with stirring to a solution of di-tert-butyl di-carbonate (820 mg, 3.7 mmol, 1.1 eq) and NaHCO<sub>3</sub> (720 mg, 8.5 mmol, 2.5 eq) in MeOH:THF:water (1:2:2) mixture at room temperature. After the reaction mixture was stirred for 6 h, the solvent mixture was evaporated. The residue was dissolved in 50 mL DCM and washed with 1% HCl (25 mL) and brine (25 mL) and then dried (MgSO<sub>4</sub>) (Yield: 0.87 g, 90%). <sup>1</sup>H NMR (600 MHz, CDCl<sub>3</sub>): 1.49 (9H, s, *t*-butyl), 3.90 (6H, s, OCH<sub>3</sub>), 5.52 (1H, s, OH), 6.54 (2H, s, ArH). <sup>13</sup>C NMR (150 MHz, CDCl<sub>3</sub>): 28.4, 45.0, 56.4, 98.4, 99.5, 104.3, 130.1, 134.0, 147.1, 156.0. MS (ESI+): C<sub>14</sub>H<sub>21</sub>NO<sub>5</sub> + Na<sup>+</sup> Calcd, 306.1. found: 305.9. Anal. Calcd. (%): C, 59.35; H, 7.47; N, 4.94. Found (%): C, 59.26; H, 7.35; N, 4.89.

#### 4.4. Synthesis of tert-butyl 4-((20-azido-3,6,9,12,15,18-hexaoxaicosyl)oxy)3,5-diiodo benzyl carbamate (3a)

K<sub>2</sub>CO<sub>3</sub> (580 mg, 4.2 mmol, 2 eq) was added with stirring to a solution of 2a (1000 mg, 2.1 mmol, 1 eq) in ACN (150 mL) at room temperature. After the reaction mixture was stirred at 80 °C for 30 min, Br-PEG6-N<sub>3</sub> (870 mg, 2.1 mmol, 1.05 eq) was added to the mixture and reaction mixture was refluxed for 24 h at 80 °C. It was filtered to remove K<sub>2</sub>CO<sub>3</sub>. Solvents were removed under reduced pressure, and the oily residue was purified with column chromatography [SiO<sub>2</sub>: DCM :MeOH (95:5)] to afford 3a as a colorless oil (Yield: 1.45 g, 85%). <sup>1</sup>H NMR (600 MHz, CDCl<sub>3</sub>): 1.48 (9H, s, *t*-butyl), 3.40 (2H, t, —CH<sub>2</sub>—N<sub>3</sub>), 3.67–3.73 (20H, m, PEG), 3.81 (2H, s, PEG), 3.98 (2H, s, PEG), 4.15 (2H, s, PEG), 4.21 (2H, s, —CH<sub>2</sub>—), 7.68 (2H, s, ArH). <sup>13</sup>C NMR (150 MHz, CDCl<sub>3</sub>): 28.4, 42.6, 50.7, 70.0, 70.1, 70.6, 70.7, 70.8, 70.9, 72.2, 79.9, 90.8, 138.2, 155.3, 156.1. MS (ESI+): C<sub>26</sub>H<sub>42</sub>I<sub>2</sub>N<sub>4</sub>O<sub>9</sub> + H<sup>+</sup> Calcd, 809.1. Anal. Calcd. (%): C, 38.63; H, 5.24; N, 6.93. Found (%): C, 38.70; H, 5.35; N, 6.85.

#### 4.5. Synthesis of tert-butyl 4-((20-azido-3,6,9,12,15,18-hexaoxaicosyl)oxy)3,5-dimethoxy benzyl carbamate (3b)

K<sub>2</sub>CO<sub>3</sub> (700 mg, 5.1 mmol, 3 eq) was added with stirring to a solution of tert-butoxycarbonyl-4-hydroxy-3,5-dimethoxybenzylamine (2b) (500 mg, 1.7 mmol, 1 eq) in ACN (150 mL) at room temperature. After the reaction mixture was stirred at 80 °C for 30 min, Br-PEG6-N<sub>3</sub> (730 mg, 1.8 mmol, 1.05 eq) was added to the mixture and reaction mixture was refluxed for 24 h at 80 °C. It was filtered to remove K<sub>2</sub>CO<sub>3</sub>. Solvents were removed under reduced pressure, and the oily residue was purified with column chromatography [SiO<sub>2</sub>: DCM:MeOH (95:5)] to afford 3b as a colorless oil (Yield: 0.7 g, 65%). <sup>1</sup>H NMR (600 MHz, CDCl<sub>3</sub>): 1.49 (9H, s, *t*-butyl), 3.41 (2H, t, —CH<sub>2</sub>—N<sub>3</sub>), 3.63 (2H, s, PEG), 3.67–3.71 (20H, m, PEG), 3.74 (2H, m, PEG), 3.85 (6H, s, OCH<sub>3</sub>), 4.14 (2H, m, PEG), 4.26

(2H, s, —CH<sub>2</sub>—), 6.51 (2H, s, ArH). <sup>13</sup>C NMR (150 MHz, CDCl<sub>3</sub>): 28.4, 44.9, 50.7, 56.1, 61.7, 70.0, 70.2, 70.3, 70.5, 70.7, 72.3, 72.6, 79.9, 104.4, 134.7, 136.2, 153.4, 155.9. MS (ESI+): C<sub>28</sub>H<sub>48</sub>N<sub>4</sub>O<sub>11</sub> + Na<sup>+</sup> Calcd, 639.3 found: 639.7. Anal. Calcd. (%): C, 54.53; H, 7.85; N, 9.08. Found (%): C, 54.81; H, 7.35; N, 9.44.

#### 4.6. Synthesis of 4-((20-azido-3,6,9,12,15,18-hexaoxaicosyl)oxy)-3,5-diiodophenyl methanamine (4a)

Compound 3a (500 mg, 0.62 mmol) was dissolved in 3 mL anhydrous 1,4-dioxane and 3 mL HCl (4 N in dioxane) was added to it and stirred at room temperature. After 4 h, the solvent was removed under reduced pressure, and the oily residue was precipitated with stirring in diethyl ether to afford 4a as a white solid (Yield: 394 mg, 90%). <sup>1</sup>H NMR (600 MHz, CDCl<sub>3</sub>): 3.44 (2H, t, —CH<sub>2</sub>—N<sub>3</sub>), 3.57 (2H, t, PEG), 3.61–3.75 (20H, s, PEG), 3.80 (2H, s, PEG), 3.96 (2H, s, PEG), 4.10 (2H, s, —CH<sub>2</sub>—), 8.06 (2H, s, ArH). <sup>13</sup>C NMR (150 MHz, CDCl<sub>3</sub>): 41.6, 50.7, 70.0, 70.2, 70.3, 70.4, 70.5, 70.6, 70.7, 72.2, 90.9, 133.2, 141.4, 158.0. MS (ESI+): C<sub>21</sub>H<sub>34</sub>I<sub>2</sub>N<sub>4</sub>O<sub>7</sub> + H<sup>+</sup> Calcd, 709.1 found: 709.0. Anal. Calcd. (%): C, 35.61; H, 4.84; N, 7.91. Found (%): C, 35.87; H, 4.33; N, 7.41.

#### 4.7. Synthesis of 4-((20-azido-3,6,9,12,15,18-hexaoxaicosyl)oxy)-3,5-dimethoxyphenyl methanamine (4b)

Compound 3b (500 mg, 0.81 mmol) was dissolved in 3 mL anhydrous 1,4-dioxane and 3 mL HCl (4 N in dioxane) was added to it and stirred at room temperature. After 4 h, the solvent was removed under reduced pressure, and the oily residue was precipitated with stirring in diethyl ether to afford 4b as a white solid that was used for the next step without further purification (Yield: 377 mg, 90%). <sup>1</sup>H NMR (600 MHz, CDCl<sub>3</sub>): 2.11 (2H, s, NH<sub>2</sub>), 3.40 (2H, t, —CH<sub>2</sub>—N<sub>3</sub>), 3.63–3.71 (20H, m, PEG), 3.76 (2H, s, PEG), 3.79 (2H, s, PEG), 3.84 (6H, s, OCH<sub>3</sub>), 4.01 (2H, s, PEG), 4.05 (2H, s, —CH<sub>2</sub>—), 6.83 (2H, s, ArH). <sup>13</sup>C NMR (150 MHz, CDCl<sub>3</sub>): 44.2, 50.7, 56.3, 70.0, 70.2, 70.1, 70.4, 70.5, 70.6, 71.8, 106.4, 129.4, 135.3, 152.6. MS (ESI+): C<sub>23</sub>H<sub>40</sub>N<sub>4</sub>O<sub>9</sub> + H<sup>+</sup> Calcd, 517.2. Anal. Calcd. (%): C, 55.08; H, 7.14; N, 9.33. Found (%): C, 54.81; H, 7.35; N, 9.44.

#### 4.8. Synthesis of N,N'-diboc-1-4-((20-azido-3,6,9,12,15,18-hexaoxaicosyl)oxy)-3,5-diiodobenzylguanidine (5a)

Compound 4a (1000 mg, 2.7 mmol, 1 eq), N,N'-Di-Boc-1H-pyrazole-1-carboxamide (840 mg, 2.7 mmol, 1 eq) was dissolved in 10 mL anhydrous DCM and then TEA (0.75 mL 5.4 mmol, 2 eq) was added to the solution. The reaction mixture was stirred at room temperature for 12 h. After completion of the reaction the solvent was removed under reduced pressure and the residue dissolved in DCM (50 mL). The organic phase was washed with 1% HCl (25 mL) and brine (25 mL) and then dried (MgSO<sub>4</sub>). The solvent was removed under reduced pressure to yield 5a, which was purified with column chromatography [SiO<sub>2</sub>: EtOAc/hexanes (2:8)] (Yield: 1140 mg, 85%). <sup>1</sup>H NMR (600 MHz, CDCl<sub>3</sub>): 1.50 (9H, s, *t*-butyl), 1.52 (9H, s, *t*-butyl), 3.40 (2H, s, —CH<sub>2</sub>—N<sub>3</sub>), 3.67–3.73 (20H, m, PEG), 3.80 (2H, m, PEG), 3.99 (2H, m, —CH<sub>2</sub>—PEG), 4.16 (2H, s, —CH<sub>2</sub>—PEG), 4.50 (2H, s, —CH<sub>2</sub>—Guanidine), 7.73 (2H, s, ArH), 8.57 (1H, s, NH). <sup>13</sup>C NMR (150 MHz, CDCl<sub>3</sub>): 28.1, 28.3, 42.6, 50.7, 70.1, 70.6, 70.9, 72.2, 79.5, 83.4, 90.8, 137.45, 139.5, 153.6, 156.1, 157.2, 163.4. MS (ESI+): C<sub>32</sub>H<sub>52</sub>I<sub>2</sub>N<sub>6</sub>O<sub>11</sub> + H<sup>+</sup> Calcd, 951.2 found: 951.0. Anal. Calcd. (%): C, 40.43; H, 5.51; N, 8.84. Found (%): C, 40.81; H, 5.38; N, 8.47.

#### 4.9. Synthesis of N,N'-diboc-1-4-((20-azido-3,6,9,12,15,18-hexaoxaicosyl)oxy)-3,5-dimethoxybenzylguanidine (5b)

Compound 4b (1000 mg, 2.7 mmol, 1 eq), N,N'-Di-Boc-1H-pyrazole-1-carboxamide (840 mg, 2.7 mmol, 1 eq) was dissolved in 10 mL anhydrous DCM and then TEA (0.75 mL 5.4 mmol, 2 eq) was added to

the solution. The reaction mixture was stirred at room temperature for 12 h. After completion of the reaction the solvent was removed under reduced pressure and the residue dissolved in DCM (50 mL). The organic phase was washed with 1% HCl (25 mL) and brine (25 mL) and then dried (MgSO<sub>4</sub>). The solvent was removed under reduced pressure to yield **5b**, which was purified with column chromatography [SiO<sub>2</sub>: EtOAc/hexanes (2:8)] (Yield: 92 mg, 80%). <sup>1</sup>H-NMR (600 MHz, CDCl<sub>3</sub>): 1.49 (9H, s, *t*-butyl), 1.52 (9H, s, *t*-butyl), 3.39 (2H, s, —CH<sub>2</sub>—N<sub>3</sub>), 3.66–3.73 (20H, m, PEG), 3.80 (2H, m, PEG), 3.84 (2H, s, —CH<sub>2</sub>—PEG), 3.92 (6H, s, —OCH<sub>3</sub>), 4.13 (2H, s, —CH<sub>2</sub>—PEG), 4.54 (2H, s, —CH<sub>2</sub>—Guanidine), 6.56 (2H, s, ArH), 8.57 (1H, s, NH). <sup>13</sup>C NMR (150 MHz, CDCl<sub>3</sub>): 28.1, 28.3, 45.3, 50.7, 56.1, 70.1, 70.3, 70.6, 72.2, 77.0, 79.4, 83.2, 103.8, 105.2, 106.7, 132.9, 136.4, 153.4, 156.2, 163.6. MS (ESI+): C<sub>34</sub>H<sub>58</sub>N<sub>6</sub>O<sub>13</sub> + H<sup>+</sup> Calcd, 759.4. Anal. Calcd. (%): C, 53.81; H, 7.70; N, 11.07. Found (%): C, 54.10; H, 7.44; N, 11.73.

**4.10. Synthesis of 2-(4-(4-((1-(20-(4-(2,3-bis(*tert*-butoxycarbonyl)guanidino)methyl)-2,6-diiodophenoxy)-3,6,9,12,15,18-hexaoxaicosyl)-1H-1,2,3-triazol-4-yl)methoxy)-3,5-diiodophenoxy)-3,5-diiodophenyl)acetic acid (6a)**

Compound **5a** (100 mg, 1 eq) and 1 eq of PGT were dissolved in 20 mL THF and stirred for 5 min, then 0.5 eq of NaAscorbate and 0.5 eq of Cu<sub>2</sub>SO<sub>4</sub> in 2 mL water were added to the mixture and stirred for 24 h at rt. After 24 h, the solvents were removed under reduced pressure to yield **6a**, which was purified with column chromatography. [SiO<sub>2</sub>: DCM/MeOH (95:5)] (Yield: 138 mg, 65%). <sup>1</sup>H NMR (600 MHz, CDCl<sub>3</sub>): 1.50 (9H, s, *t*-butyl), 1.52 (9H, s, *t*-butyl), 3.60 (2H, s, —CH<sub>2</sub>—PEG), 3.63 (20H, m, PEG), 3.72 (2H, s, —CH<sub>2</sub>—), 3.81 (2H, s, —CH<sub>2</sub>—), 3.90 (2H, s, —CH<sub>2</sub>—), 3.99 (2H, s, CH<sub>2</sub>—COOH), 4.49 (2H, s, —CH<sub>2</sub>—Guanidine), 4.60 (2H, s, —CH—), 5.20 (2H, s, Triazole—CH<sub>2</sub>—O), 7.22 (2H, s, ArCH) 7.72 (2H, d, ArH), 7.82 (2H, d, ArCH), 8.04 (1H, s, CH), 8.59 (1H, s, NH), 11.51 (1H, s, COOH). <sup>13</sup>C NMR (150 MHz, CDCl<sub>3</sub>): 28.1, 28.3, 39.1, 42.6, 50.4, 66.6, 69.5, 70.1, 70.5, 70.6, 70.9, 72.2, 77.7, 79.7, 83.5, 90.6, 90.9, 124.9, 126.5, 135.3, 137.2, 139.5, 141.2, 143.2, 152.5, 156.1, 157.2, 163.3, 172.6. MS (ESI+): C<sub>49</sub>H<sub>62</sub>I<sub>6</sub>N<sub>6</sub>O<sub>15</sub> + H<sup>+</sup> Calcd, 1736.9 found: 1737.1. Anal. Calcd. (%): C, 33.89; H, 3.60; N, 4.84. Found (%): C, 33.11; H, 3.22; N, 5.17.

**4.11. Synthesis of 2-(4-(4-((1-(20-(4-(2,3-bis(*tert*-butoxycarbonyl)guanidino)methyl)-2,6-dimethoxyphenoxy)-3,6,9,12,15,18-hexaoxaicosyl)-1H-1,2,3-triazol-4-yl)methoxy)-3,5-diiodophenoxy)-3,5-diiodophenyl)acetic acid (6b)**

Compound **5b** (100 mg, 1 eq) and 1 eq of PGT were dissolved in 20 mL THF and stirred for 5 min, then 0.5 eq of NaAscorbate and 0.5 eq of Cu<sub>2</sub>SO<sub>4</sub> in 2 mL water were added to the mixture and stirred for 24 h at rt. After 24 h, the solvents were removed under reduced pressure to yield **6b**, which was purified with column chromatography. [SiO<sub>2</sub>: DCM/MeOH (95:5)] (Yield: 142 mg, 70%). <sup>1</sup>H NMR (600 MHz, CDCl<sub>3</sub>): 1.49 (9H, s, *t*-butyl), 1.52 (9H, s, *t*-butyl), 3.59 (2H, s, —CH<sub>2</sub>—PEG), 3.62–3.74 (20H, m, —CH<sub>2</sub>—PEG), 3.81 (2H, s, —CH<sub>2</sub>—PEG), 3.84 (6H, s, —OCH<sub>3</sub>), 3.90 (2H, s, —CH<sub>2</sub>—PEG), 4.14 (2H, s, —CH<sub>2</sub>—PEG), 4.52 (2H, s, CH<sub>2</sub>—COOH), 4.59 (2H, s, —CH<sub>2</sub>—Guanidine), 5.20 (2H, s, Triazole—CH<sub>2</sub>—O), 6.56 (2H, s, ArCH) 7.22 (2H, s, ArH), 7.82 (2H, d, ArCH), 8.03 (1H, s, Triazole CH), 8.60 (1H, s, NH). <sup>13</sup>C NMR (150 MHz, CDCl<sub>3</sub>): 28.1, 28.3, 39.3, 45.3, 50.4, 56.1, 66.7, 69.5, 70.6, 72.2, 77.7, 79.5, 83.3, 90.6, 105.2, 124.9, 126.5, 132.9, 135.7, 136.4, 141.2, 143.3, 152.3, 152.9, 153.4, 156.1, 163.4, 172.5. MS (ESI+): C<sub>51</sub>H<sub>68</sub>I<sub>4</sub>N<sub>6</sub>O<sub>17</sub> + H<sup>+</sup> Calcd, 1545.1. Anal. Calcd. (%): C, 39.65; H, 4.44; N, 5.44. Found (%): C, 39.10; H, 4.12; N, 5.88.

**4.12. Synthesis of 2-(4-(4-((1-(20-(4-(guanidinomethyl)-2,6-diiodophenoxy)-3,6,9,12,15,18-hexaoxaicosyl)-1H-1,2,3-triazol-4-yl)methoxy)-3,5-diiodophenoxy)-3,5-diiodophenyl)acetic acid (7a)**

Compound **6a** (100 mg) was dissolved in 3 mL anhydrous 1,4-dioxane and 9 mL HCl (4 N in dioxane) was added to it and stirred at rt. After 24 h the solvent was removed under reduced pressure, and the oily residue was precipitated with diethyl ether to afford **7a** as a white powder which was purified with RP column chromatography. [C18: MeOH/Water (70:30)] (Yield: 60 mg, 70%). Purity > 98%, t<sub>R</sub> = 17.1 min [analytical HPLC/gradient: 50–95% MeOH in H<sub>2</sub>O (0.1% TFA), 50 min, flow rate 1 mL/min, Pursuit XRs C18 column (150 × 4.6 mm)]. <sup>1</sup>H NMR (600 MHz, DMSO): 3.51 (2H, s, —CH<sub>2</sub>—PEG), 3.60–3.68 (20H, s, —CH<sub>2</sub>—PEG), 3.76 (2H, s, CH<sub>2</sub>—COOH), 3.91 (2H, s, CH<sub>2</sub>—PEG), 3.95 (2H, s, —CH<sub>2</sub>—PEG), 4.27 (2H, s, —CH<sub>2</sub>—PEG), 4.60 (2H, s, Ar-CH<sub>2</sub>—Guanidine), 5.14 (2H, s, Triazole—CH<sub>2</sub>—O), 7.60 (2H, s, ArH Guanidine), 7.76 (2H, s, ArCH-TAT), 7.84 (2H, s, ArCH-TAT), 8.09 (1H, s, NH), 8.24 (1H, s, Triazole CH), 9.45 (1H, s, COOH). <sup>13</sup>C NMR (150 MHz, CDCl<sub>3</sub>): 39.9, 42.1, 50.0, 66.4, 69.1, 69.7, 70.3, 71.9, 90.1, 90.4, 90.8, 124.8, 126.1, 137.1, 138.4, 140.8, 142.7, 150.9, 152.1, 152.8, 156.6, 157.7, 164.3, 174.7. MS (ESI+): C<sub>39</sub>H<sub>46</sub>I<sub>6</sub>N<sub>6</sub>O<sub>11</sub> + H<sup>+</sup> Calcd, 1536.2 found: 1535.6. Anal. Calcd. (%): C, 30.49; H, 3.02; N, 5.47. Found (%): C, 30.11; H, 3.48; N, 5.79.

**4.13. Synthesis of 2-(4-(4-((1-(20-(4-(guanidinomethyl)-2,6-diiodophenoxy)-3,6,9,12,15,18-hexaoxaicosyl)-1H-1,2,3-triazol-4-yl)methoxy)-3,5-diiodophenoxy)-3,5-dimethoxyphenyl)acetic acid (7b)**

Compound **6b** (100 mg) was dissolved in 3 mL anhydrous 1,4-dioxane and 9 mL HCl (4 N in dioxane) was added to it and stirred at rt. After 24 h the solvent was removed under reduced pressure, and the oily residue was precipitated with diethyl ether to afford **7b** as a white powder, which was purified with RP column chromatography. [C18: MeOH/Water (70:30)] (Yield: 61 mg, 70%). Purity > 98%, t<sub>R</sub> = 13.5 min [analytical HPLC/gradient: 50–95% MeOH in H<sub>2</sub>O (0.1% TFA), 50 min, flow rate 1 mL/min, Pursuit XRs C18 column (150 × 4.6 mm)]. <sup>1</sup>H NMR (600 MHz, DMSO): 3.36 (2H, s, —CH<sub>2</sub>—PEG), 3.50 (2H, s, —CH<sub>2</sub>—PEG), 3.58–3.67 (20H, s, —CH<sub>2</sub>—PEG), 3.74 (2H, s, —CH<sub>2</sub>—PEG), 3.82 (6H, s, —OCH<sub>3</sub>), 3.90 (2H, s, —CH<sub>2</sub>—PEG), 4.08 (2H, s, CH<sub>2</sub>—COOH), 4.60 (2H, s, —CH<sub>2</sub>—Guanidine), 5.40 (2H, s, Triazole—CH<sub>2</sub>—O), 6.59 (2H, s, ArCH) 7.63 (2H, s, ArH), 7.83 (2H, d, ArCH), 8.09 (1H, s, Triazole CH), 8.25 (1H, s, NH), 9.28 (1H, s, COOH). <sup>13</sup>C NMR (150 MHz, CDCl<sub>3</sub>): 44.8, 47.1, 49.6, 50.0, 58.5, 60.9, 71.3, 74.1, 75.2, 76.8, 82.6, 95.0, 95.4, 109.2, 129.8, 131.1, 137.6, 140.8, 144.0, 145.8, 147.7, 155.9, 157.1, 157.8, 162.9, 169.3, 179.7. MS (ESI+): C<sub>41</sub>H<sub>52</sub>I<sub>4</sub>N<sub>6</sub>O<sub>13</sub> + H<sup>+</sup> Calcd, 1345.0, found 1344.7. Anal. Calcd. (%): C, 36.63; H, 3.90; N, 6.25. Found (%): C, 36.18; H, 4.48; N, 6.48.

**4.14. Synthesis of *tert*-butoxycarbonyl-4-hydroxybenzylamine (9)**

4-Hydroxybenzylamine (**8**) (0.62 g, 5 mmol) was slowly added with stirring to di-*tert*-butyl di-carbonate (1.2 g, 5.1 mmol) at rt. After the reaction mixture was stirred for 4 h, the oily residue was purified with column chromatography [SiO<sub>2</sub>: EtOAc/hexanes (1:4)] to afford 0.82 g of *N*-Boc-4-hydroxybenzylamine (**9**) as a colorless oil (Yield: 53 mg, 71%). <sup>1</sup>H NMR (600 MHz, CDCl<sub>3</sub>): 1.49 (9H, s, *t*-butyl), 4.26 (2H, s, —CH<sub>2</sub>—), 4.89 (1H, s, NH), 5.76 (1H, s, —OH), 6.79 (2H, d, ArH), 7.14 (2H, d, ArH). <sup>13</sup>C NMR (150 MHz, CDCl<sub>3</sub>): 22.7, 28.4, 44.2, 45.5, 79.7, 115.5, 121.4, 128.9, 130.6, 155.2, 156.0. MS (ESI+): C<sub>12</sub>H<sub>17</sub>NO<sub>3</sub> Calcd 223.1. Anal. Calcd. (%): C, 64.55; H, 7.67; N, 6.20. Found (%): C, 64.71; H, 7.51; N, 5.99.

**4.15. Synthesis of *tert*-butyl 4-((23-hydroxy-3,6,9,12,15,18,21-heptaooxatricosyl)oxy)benzyl carbamate (10)**

K<sub>2</sub>CO<sub>3</sub> (478 mg, 3.5 mmol, 3 eq) was added with stirring to a solution

of *tert*-butoxycarbonyl-4-hydroxybenzylamine (**9**) (280 mg, 1.2 mmol, 1 eq) in ACN (25 mL) at rt. After the reaction mixture was stirred for 30 min, Br-PEG7-OH (500 mg, 1.2 mmol, 1 eq) was added to mixture and then refluxed for 24 h. It was filtered to remove excess  $K_2CO_3$ . Solvents were removed under reduced pressure, and the oily residue was purified with column chromatography [SiO<sub>2</sub>:DCM:MeOH (95:5)] to afford **10** as a yellow oil (Yield: 530 mg, 80%). <sup>1</sup>H NMR (600 MHz, CDCl<sub>3</sub>): 1.48 (9H, s, *t*-butyl), 3.62 (2H, s, —CH<sub>2</sub>—OH), 3.66–3.70 (24H, m, —CH<sub>2</sub>—CH<sub>2</sub>—PEG), 3.74 (2H, s, —CH<sub>2</sub>—PEG), 3.87 (2H, s, —CH<sub>2</sub>—PEG), 4.13 (2H, s, —CH<sub>2</sub>—PEG), 4.26 (2H, s, —CH<sub>2</sub>—), 4.84 (1H, s, NH), 6.89 (2H, d, ArCH), 7.21 (2H, d, ArCH). <sup>13</sup>C NMR (150 MHz, CDCl<sub>3</sub>): 28.4, 44.2, 61.7, 67.4, 69.7, 70.3, 70.5, 70.6, 70.8, 72.6, 114.7, 128.3, 131.2, 155.9, 158.3. MS (ESI+): C<sub>28</sub>H<sub>49</sub>NO<sub>11</sub> + NH<sub>4</sub><sup>+</sup> Calcd 593.3, found 593.2. Anal. Calcd. (%): C, 58.42; H, 8.58; N, 2.43. Found (%): C, 58.81; H, 8.11; N, 2.91.

Synthesis of 23-(4-(((*tert*-butoxycarbonyl)amino)methyl)phenoxy)-3,6,9,12,15,18,21-heptaaxatricosyl 4-methylbenzenesulfonate (**11**)

To a solution of the **10** (150 mg, 0.26 mmol) in DCM (20 mL) at 0 °C was added TEA (0.15 mL, 1.04 mmol) followed by TosCl (150 mg, 0.78 mmol). The reaction mixture was stirred at 0 °C for 30 min, then was allowed to warm to rt over 2 h. The mixture was quenched with H<sub>2</sub>O (10 mL) and extracted with DCM (2 × 50 mL). The combined organics were washed with H<sub>2</sub>O (50 mL), brine (50 mL), dried (Na<sub>2</sub>SO<sub>4</sub>), and concentrated. The resulting material was purified with column chromatography [SiO<sub>2</sub>: DCM:MeOH (95:5)] to provide **11** as a white powder (Yield: 150 mg, 79%). <sup>1</sup>H NMR (600 MHz, CDCl<sub>3</sub>): 1.47 (9H, s, *t*-butyl), 2.46 (3H, s, —CH<sub>3</sub>), 3.62 (2H, s, —CH<sub>2</sub>—PEG), 3.66–3.73 (24H, s, —CH<sub>2</sub>—PEG), 3.86 (2H, s, —CH<sub>2</sub>—PEG), 4.12 (2H, s, —CH<sub>2</sub>—PEG), 4.17 (2H, s, —CH<sub>2</sub>—PEG), 4.25 (2H, s, —CH<sub>2</sub>—), 6.87 (2H, d, ArCH), 7.20 (2H, d, ArH), 7.35 (2H, d, ArCH), 7.80 (2H, d, ArH). <sup>13</sup>C NMR (150 MHz, CDCl<sub>3</sub>): 21.6, 28.4, 43.4, 44.1, 61.5, 67.4, 68.6, 69.2, 69.7, 70.4, 70.6, 70.7, 70.8, 72.6, 90.6, 91.2, 114.7, 126.3, 127.9, 128.8, 129.8, 131.2, 131.9, 139.6, 144.8, 155.8, 158.1, 190.8. MS (ESI+): C<sub>35</sub>H<sub>55</sub>NO<sub>13</sub>S + NH<sub>4</sub><sup>+</sup> Calcd, 747.4 found: 747.8. Anal. Calcd. (%): C, 57.60; H, 7.60; N, 1.92. Found (%): C, 57.12; H, 7.32; N, 1.66.

#### 4.16. Synthesis of methyl 2-(4-(3,5-diiodo-4-(3-(piperazin-1-yl)propoxy)phenoxy)-3,5-diiodophenyl) acetate (**19**)

In a 2-neck flask, the methyl ester of tetrac (1 g, 1.3 mmol) and Cs<sub>2</sub>CO<sub>3</sub> (1 g, 3.25 mmol) were stirred in 50 mL ACN at 60 °C. After 30 min *tert*-butyl 4-(3-(methanesulfonyloxy)propyl)piperazine-1-carboxylate hydrochloride (**18**) (0.47 g, 1.3 mmol) was added to the flask and refluxed for 18 h. After completion of the reaction, it was filtered to remove the Cs<sub>2</sub>CO<sub>3</sub>. Solvents were removed under reduced pressure. The residue was dissolved in 5 mL anhydrous 1,4-dioxane and 5 mL HCl (4 N in dioxane) was added to it and stirred at rt. After 2 h the solvent was removed under reduced pressure, and the residue was precipitated with diethyl ether to afford **19** as a white powder that was used for the next step without further purification (Yield: 860 mg, 75%). <sup>1</sup>H NMR (600 MHz, DMSO): 2.77 (4H, m, N—CH<sub>2</sub>—CH<sub>2</sub>—N), 2.94 (4H, m, N—CH<sub>2</sub>—CH<sub>2</sub>—N), 3.59 (2H, s, —CH<sub>2</sub>—CH<sub>2</sub>—), 3.62 (3H, s, —OCH<sub>3</sub>), 3.73 (2H, s, ArCH<sub>2</sub>—), 3.86 (2H, s, —CH<sub>2</sub>—), 4.13 (2H, s, —CH<sub>2</sub>—), 7.32 (2H, s, ArCH-TAT), 8.04 (2H, s, ArCH-TAT). <sup>13</sup>C NMR (150 MHz, CDCl<sub>3</sub>): 29.3, 34.3, 34.4, 37.9, 48.1, 51.7, 53.9, 70.3, 90.6, 91.2, 136.9, 141.7, 152.2, 153.2, 161.9, 171.2. MS (ESI+): C<sub>22</sub>H<sub>24</sub>I<sub>4</sub>N<sub>2</sub>O<sub>4</sub> + H<sup>+</sup> Calcd, 888.8 found: 888.8. Anal. Calcd. (%): C, 29.75; H, 2.72; N, 3.15. Found (%): C, 29.63; H, 2.59; N, 3.76.

#### 4.17. Synthesis of methyl 2-(4-(4-(3-(4-(23-(4-(((*tert*-butoxycarbonyl)amino)methyl)phenoxy)-3,6,9,12,15,18,21-heptaaxatricosyl)piperazin-1-yl)propoxy)-3,5-diiodophenoxy)-3,5-diiodophenyl)acetate (**12**)

Compound **11** (100 mg, 0.14 mmol, 1 eq), **17** (120 mg, 0.14 mmol, 1 eq) and K<sub>2</sub>CO<sub>3</sub> (90 mg, 0.55 mmol, 1 eq) were refluxed with 30 mL ACN for 18 h. After completion of the reaction, it was filtered to remove the K<sub>2</sub>CO<sub>3</sub>. Solvents were removed under reduced pressure, and the oily

residue was purified with reverse phase chromatography. [C18: MeOH/Water (55:45)] (Yield: 118 mg, 60%). <sup>1</sup>H NMR (600 MHz, DMSO): 1.47 (9H, s, *t*-butyl), 2.12 (2H, t, CH<sub>2</sub>) 2.63–2.67 (8H, m, N-CH<sub>2</sub>—CH<sub>2</sub>—N), 3.59 (2H, s, —CH<sub>2</sub>—), 3.61–3.70 (24H, m, PEG—CH<sub>2</sub>—), 3.73 (2H, s, —CH<sub>2</sub>—), 3.76 (3H, s, —OCH<sub>3</sub>), 3.86 (2H, s, —CH<sub>2</sub>—), 4.02 (2H, s, —CH<sub>2</sub>—), 4.12 (2H, s, —CH<sub>2</sub>—), 4.24 (2H, s, —CH<sub>2</sub>—), 6.88 (2H, d, ArH), 7.18 (2H, s, ArH—Tetrac), 7.20 (2H, d, ArH), 7.79 (2H, s, ArH—Tetrac). <sup>13</sup>C NMR (150 MHz, CDCl<sub>3</sub>): 27.3, 28.4, 39.2, 44.2, 52.5, 52.9, 53.5, 55.0, 57.7, 67.5, 68.8, 69.8, 70.4, 70.5, 70.8, 71.7, 90.3, 90.6, 114.7, 126.4, 128.8, 135.2, 141.1, 152.5, 153.2, 155.9, 158.1, 170.7. MS (ESI+): C<sub>50</sub>H<sub>71</sub>I<sub>4</sub>N<sub>3</sub>O<sub>14</sub> + H<sup>+</sup> Calcd, 1446.1 found: 1445.9. Anal. Calcd. (%): C, 41.54; H, 4.95; N, 2.91. Found (%): C, 41.14; H, 4.55; N, 2.21.

#### 4.18. Synthesis of methyl 2-(4-(4-(3-(4-(23-(4-(aminomethyl)phenoxy)-3,6,9,12,15,18,21-heptaaxatricosyl)piperazin-1-yl)propoxy)-3,5-diiodophenoxy)-3,5-diiodophenyl) acetate (**13**)

Compound **12** (100 mg) was dissolved in 3 mL anhydrous 1,4-dioxane and 6 mL HCl (4 N in dioxane) was added to it and stirred at rt. After 24 h the solvent was removed under reduced pressure, and the oily residue was precipitated with diethyl ether to afford compound **13** as a white powder that was used for the next step without further purification (Yield: 90 mg, 96%). <sup>1</sup>H NMR (600 MHz, DMSO): 1.98 (2H, s, —CH<sub>2</sub>—), 3.52–3.55 (28H, m, —CH<sub>2</sub>—PEG), 3.57 (3H, s, —OCH<sub>3</sub>), 3.58 (8H, m, N—CH<sub>2</sub>—CH<sub>2</sub>—N), 3.65 (2H, s, CH<sub>2</sub>—COOCH<sub>3</sub>), 3.75 (2H, s, —CH<sub>2</sub>—), 3.84 (2H, s, Ar—CH<sub>2</sub>—), 3.95 (2H, m, —CH<sub>2</sub>—), 6.99 (2H, s, ArH Guanidine), 7.17 (2H, s, ArCH-TAT), 7.42 (2H, s, ArH Guanidine), 7.88 (2H, s, ArCH-TAT), 8.34 (1H, s, NH). <sup>13</sup>C NMR (150 MHz, CDCl<sub>3</sub>): 38.74, 52.6, 56.9, 67.8, 69.5, 81.6, 83.31, 83.38, 84.1, 106.1, 128.9, 139.9, 140.4, 144.9, 155.4, 165.9, 167.2, 172.9, 186.4. MS (ESI+): C<sub>45</sub>H<sub>63</sub>I<sub>4</sub>N<sub>3</sub>O<sub>12</sub> + H<sup>+</sup> Calcd, 1346.1 found: 1345.7. Anal. Calcd. (%): C, 40.17; H, 4.72; N, 3.12 Found (%): C, 40.56; H, 5.12; N, 3.51.

#### 4.19. Synthesis of methyl 2-(4-(4-(3-(4-(23-(4-((2,3-bis(*tert*-butoxycarbonyl)guanidino)methyl)phenoxy)-3,6,9,12,15,18,21-heptaaxatricosyl)piperazin-1-yl)propoxy)-3,5-diiodophenoxy)-3,5-diiodophenyl) acetate (**14**)

Compound **13** (120 mg, 0.09 mmol, 1 eq), *N,N*-Di-Boc 1H-pyrazole-1-carboxamide (33 mg, 0.11 mmol, 1.2 eq) was dissolved in 5 mL anhydrous DCM and then TEA (25 μL, 0.18 mmol, 2 eq) was added to the solution. The reaction mixture was stirred at room temperature for 18 h. After completion of the reaction the solvent was removed under reduced pressure and the residue dissolved in DCM (30 mL). The organic phase washed with 1% HCl (25 mL) and brine (25 mL) and then dried (MgSO<sub>4</sub>). The solvent was removed under reduced pressure to yield **14**, which was purified with column chromatography [SiO<sub>2</sub>: DCM:MeOH (95:5)] (Yield: 120 mg, 85%). <sup>1</sup>H NMR (600 MHz, DMSO): 1.39 (9H, s, *t*-butyl), 1.52 (9H, s, *t*-butyl), 1.97 (2H, s, —CH<sub>2</sub>—CH<sub>2</sub>—), 2.51–2.67 (8H, m, N—CH<sub>2</sub>—CH<sub>2</sub>—N), 3.49–3.51 (24H, m, —CH<sub>2</sub>—PEG), 3.54 (2H, s, —CH<sub>2</sub>—), 3.57 (2H, s, —CH<sub>2</sub>—), 3.64 (3H, s, —OCH<sub>3</sub>), 3.72 (2H, m, —CH<sub>2</sub>—), 3.74 (2H, m, —CH<sub>2</sub>—), 3.90 (2H, s, —CH<sub>2</sub>—PEG), 4.06 (2H, s, CH<sub>2</sub>—COOCH<sub>3</sub>), 4.43 (2H, s, Ar-CH<sub>2</sub>-Guanidine), 6.92 (2H, s, ArH Guanidine), 7.14 (2H, s, ArCH-TAT), 7.21 (2H, s, ArH Guanidine), 7.88 (2H, s, ArCH-TAT), 8.54 (1H, s, NH). <sup>13</sup>C NMR (150 MHz, CDCl<sub>3</sub>): 28.3, 42.9, 44.5, 44.9, 52.3, 52.9, 54.8, 57.4, 67.4, 68.4, 69.7, 70.3, 70.5, 70.8, 71.4, 79.3, 83.9, 90.2, 114.8, 126.4, 129.1, 141.9, 151.1, 155.9, 158.3, 164.6, 175.9. MS (ESI+): C<sub>56</sub>H<sub>81</sub>I<sub>4</sub>N<sub>5</sub>O<sub>16</sub> + H<sup>+</sup> Calcd, 1588.2 found: 1588.2. Anal. Calcd. (%): C, 42.36; H, 5.14; N, 4.41. Found (%): C, 42.24; H, 5.22; N, 4.48.

4.20. *Synthesis of 2-(4-(4-(3-(4-(23-(4-(guanidinomethyl)phenoxy)-3,6,9,12,15,18,21-heptaaxatricosyl)piperazin-1-yl)propoxy)-3,5-diiodophenoxy)-3,5-diiodophenyl)acetic acid (15)*

Compound **14** (100 mg) was dissolved in 3 mL 1,4-dioxane:water (3:1) and 3 mL conc. HCl added to it and stirred at rt. After 24 h the solvent was removed under reduced pressure, and the oily residue was precipitated with diethyl ether to afford compound **15** as a white powder, which was purified with reverse phase column chromatography. [C18: MeOH/Water (55:45)] (Yield: 60 mg, 70%). Purity > 98%, t<sub>R</sub> = 27.5 min [analytical HPLC/gradient: 50–95% MeOH in H<sub>2</sub>O (0.1% TFA), 50 min, flow rate 1 mL/min, Pursuit XRs C18 column (150 × 4.6 mm)]. <sup>1</sup>H NMR (600 MHz, DMSO): 2.09 (2H, m, –CH<sub>2</sub>–CH<sub>2</sub>–), 2.58 (2H, m, –CH<sub>2</sub>–CH<sub>2</sub>–), 2.65 (8H, m, N–CH<sub>2</sub>–CH<sub>2</sub>–N), 3.20 (2H, s, –CH<sub>2</sub>–CH<sub>2</sub>–), 3.51 (2H, s, CH<sub>2</sub>–COOH), 3.55–3.62 (24H, m, –CH<sub>2</sub>–PEG), 3.69 (2H, s, –CH<sub>2</sub>–PEG), 3.83 (2H, s, –CH<sub>2</sub>–PEG), 3.99 (2H, s, –CH<sub>2</sub>–PEGCH<sub>2</sub>–PEG), 4.10 (2H, s, –CH<sub>2</sub>–PEG), 4.26 (2H, s, Ar–CH<sub>2</sub>–Guanidine), 6.89 (2H, s, ArH Guanidine), 7.15 (2H, s, ArH Guanidine), 7.58 (2H, s, ArCH–TAT), 7.81 (2H, s, ArCH–TAT), 8.23 (1H, s, NH), 8.73 (1H, s, COOH). <sup>13</sup>C NMR (150 MHz, CDCl<sub>3</sub>): 26.7, 39.9, 41.2, 44.1, 52.2, 52.7, 54.4, 57.1, 67.2, 68.2, 69.3, 70.2, 71.3, 90.1, 114.6, 126.1, 128.4, 138.1, 140.9, 151.1, 152.7, 157.7, 158.1, 164.4, 173.9. MS(ESI<sup>+</sup>): C<sub>45</sub>H<sub>63</sub>L<sub>4</sub>N<sub>5</sub>O<sub>12</sub> + H<sup>+</sup> Calcd, 1373.9 found:1373.5. Anal. Calcd. (%): C, 39.35; H, 4.62; N, 5.10. Found (%): C, 39.12; H, 4.89; N, 5.67.

#### 4.21. Biological Materials

Bovine serum albumin (BSA) and fetal bovine serum (FBS) were purchased from Sigma-Aldrich, anti- $\alpha\beta 3$  was purchased from Bioss Inc., streptavidin HRP conjugate was from ThermoFischer Scientific, and Iscove's Modified Dulbecco's Medium (IMDM) was from Hyclon. GraphPad Prism software was used for calculation of IC<sub>50</sub> values.

### 5. LC-MS/MS instrumentation

An API-4000 mass spectrometer (Sciex, Framingham, MA) equipped with a Shimadzu UPLC system (Kyoto, Japan) was used for LC-MS/MS analyses. A Kinetex 2.6  $\mu$ m Biphenyl 100 LS column (50 × 2.1 mm, Phenomenex, Torrance, CA) was used for reversed-phase separation. Mobile phases were (A) water containing 0.1% formic acid and 5% acetonitrile and (B) acetonitrile. The flow rate was 0.35 mL/min, and the gradient was linear from 25% B to 95% B for 2–4 min. The oven temperature was 40 °C and the injection volume was 5  $\mu$ L. Electro-spray ionization (ESI) was used in positive MRM mode. Mass transitions for analytes were: Q1/Q3: 1285.0/133.0 (BG-P<sub>400</sub>-TAT); 1535.0/291.1 (**7a**); 1344.9/139.2 (**7b**); 1374.3/89.0 (**15**); 1343.3/1225.9 (**20**); 275.09/275.5 (MIBG). The operative parameters of the mass spectrometer were as follows: declustering potentials (DP): 75 V; entrance potentials (EP): 10; collision energies (CE): 90 eV; collision cell exit potential (CXP), 8 V; curtain gas (CUR), 30 psi; gas 1 (GS1, nebulizer gas) 30 psi; gas 2 (GS2, heater gas) 30 psi; ion spray voltage (IS), 5000 V; temperature (TEM), 500 °C; collision activate dissociation (CAD) gas: 12 psi; dwell time: 150 ms. Nitrogen was used for the gases. Standard curves were obtained using standard solutions of the analytes with concentrations of 1000, 300, 100, 30, 10, 3, and 1 ng/mL. The regression curves of the LC-MS/MS method for standard solutions was linear or quadratic ( $r = 0.99$  or more) from a concentration of 1 to 1000 ng/mL for each analyte. The LOQ was estimated to be 10 ng/mL or less under the current conditions for each analyte. Accuracy ranged 90–100%; and recovery was more than 90% or more for each analyte.

### 6. Sample preparation of cell samples with liquid–liquid extraction

Cell samples were thawed and homogenized with acetonitrile (1 mL)

with a hand homogenizer. After centrifugation, solvent was evaporated under a nitrogen stream at 50 °C. Extracts were reconstituted with 50  $\mu$ L of acetonitrile/water (80/20 v/v). Samples were immediately injected into LC-MS/MS for quantification of analytes on the same day.

#### 6.1. Cell culture

Neuroblastoma cells SK-N-F1 (ATCC) were grown with IMDM supplemented with 10% FBS, 10% penicillin, and 1% streptomycin. Cells were cultured at 37 °C to subconfluence and treated with 0.25% (w/v) trypsin/ethylenediaminetetraacetic acid (EDTA) to induce cell release from flask. The cells were washed with culture medium that was free of phenol red and fetal bovine serum and counted.

#### 6.2. Competitive binding

The binding affinities of dl-BG-P<sub>400</sub>-TAT (**7a**), dM-BG-P<sub>400</sub>-TAT (**7b**), BG-P<sub>400</sub>-PAT (**15**) and BG-P<sub>400</sub>-TAT to purified  $\alpha\beta 3$  were measured using previously described methods with slight modifications<sup>37</sup>. The purified  $\alpha\beta 3$  (1  $\mu$ g/mL) was coated to polystyrene micro-titer plate wells at 4 °C overnight, and then the wells were blocked with 3% BSA for 2 h at room temperature. Wells were washed with buffer A (50 mM Tris/HCl, 100 mM NaCl, 1 mM CaCl<sub>2</sub>, 1 mM MgCl<sub>2</sub>, 1% BSA), and anti- $\alpha\beta 3$  (conjugated with biotin 1:1000 in buffer A) was added and incubated for 1 h at room temperature. Increasing concentrations of **7a**, **7b**, and **15** were added in the presence or absence of fibrinogen and incubated for 2 h at room temperature, and then wells were washed 3 times with buffer A and incubated with a streptavidin HRP conjugate (1:1000 in buffer A) for 1 h at room temperature. Finally, wells were washed 3 times with buffer A and 100  $\mu$ L peroxidase substrate 3,3',5,5'-tetramethylbenzidine (TMB) was added, and the reaction was terminated after 30 min with 50  $\mu$ L of 450 nm stop solution for TMB. Absorbance was determined at 450 nm with a plate reader. The best-fit IC<sub>50</sub> values for the compounds were calculated by fitting the data with nonlinear regression using GraphPad Prism<sup>38</sup>.

#### 6.3. Cellular uptake of BG-P-TAT derivatives

SK-N-F1 cells were treated with MIBG, BG-P<sub>400</sub>-TAT, **7a**, **7b**, **15** and **20** at 1  $\mu$ M concentration. After 15 min, 30 min and 60 min incubation then cells were collected and washed with PBS followed by separating cells from media by centrifugation at 5,000g for 10 min.

#### 6.4. Animals

Immunodeficient female NCr nude homozygous mice aged 5–6 weeks and weighing 20–25 g were purchased from Taconic Biosciences, Inc. All animal studies were conducted at the animal facility of the Veteran Affairs (VA) Medical Center in accordance with institutional guidelines for humane animal treatment and approved by the VA IACUUC. Four mice in each group were maintained under specific pathogen-free conditions and housed under controlled conditions of temperature (20–24 °C) and humidity (60–70%) and 12 h light/dark cycle with ad libitum access to water and food. Mice were allowed to acclimatize for 5 days and injected with 2 million cells for each implant. The tumor volumes were allowed to reach 500 mm<sup>3</sup> and then compounds were administrated subcutaneously (s.c.) daily for 21 days. At the end of the study, animals were sacrificed, and tumors were collected.

#### 6.5. Histopathology analysis

Collected tumors were fixed in 10% formalin for at least 48 h. The fixed samples were placed in plastic cassettes and dehydrated using an automated tissue processor. The processed tissues were embedded in paraffin wax and blocks trimmed and sectioned to about 5 × 4  $\mu$ m size using a microtome. The tissue sections were mounted on glass slides

using a hot plate and subsequently treated in the order of 100%, 90% and 70% ethanol for 2 min each. Finally, the tissue sections were rinsed in tap water, stained with the Harris's hematoxylin and eosin (H&E), and examined under a light microscope.

### 6.6. Preparation of ligands for docking

All compounds (**7a**, **7b**, **15**) were drawn using the 2D and 3D options of Chem Draw 12.0 and saved in mol2 format. The created .pdbfile was submitted to AutoDock Vina (version 1.1.2) to set number of torsion and for .pdbqt file construction.

### 6.7. Target selection and preparation

The X-ray crystal structure of integrin  $\alpha\beta3$  (PDB:1L5G) with 3.20 Å resolution was obtained in .pdb format from the Protein Data Bank. Before performing the docking calculation, all water molecules were removed from the crystal structure, all hydrogen atoms and Gasteiger charges were added to every atom of the protein, and rotatable bonds were selected using AutoDock Tools-1.5.6. Auto grid box was generated with dimensions 50 × 50 × 50 Å with grid spacing 0.375 Å. The grid box is based on the inhibitory site residue used for the docking calculation.

### 6.8. Molecular docking

After running docking calculations, nine conformers were generated for each compound and all the conformers were ranked in a log file based on their docking score. Molecular docking interactions were analyzed using PyMOL (The PyMOL Molecular Graphics System, Version 1.7.4, Schrodinger LLC).

### Declaration of Competing Interest

The authors declare the following financial interests/personal relationships which may be considered as potential competing interests: 'S.A.M. and O.O.K are inventors on patents related to BG-P-TAT and S.A.M. is a founder of Nanopharmaceutical LLC, which is developing anti-cancer drugs. The remaining author K.G., K.F. declares no conflict of interest'.

### Acknowledgements

Funding was received from both NanoPharmaceuticals LLC, Rensselaer, NY and from the Pharmaceutical Research Institute (PRI) at Albany College of Pharmacy and Health Sciences. We thank Dr. Keating, Medical Editor/Writer at PRI for her excellent editorial review of the manuscript.

### Appendix A. Supplementary material

Supplementary data to this article can be found online at <https://doi.org/10.1016/j.bmc.2021.116250>.

### References

- Maris JM, Hogarty MD, Bagatell R, Cohn SL. Neuroblastoma. *Lancet*. 2007;369:2106–2120.
- Colon NC, Chung DH. Neuroblastoma. *Adv Pediatr*. 2011;58:297–311.
- Friedman GK, Castleberry RP. Changing trends of research and treatment in infant neuroblastoma. *Pediatr Blood Cancer*. 2007;49:1060–1065.
- Brodeur GM, Iyer R, Croucher JL, Zhuang T, Higashi M, Kolla V. Therapeutic targets for neuroblastomas. *Expert Opin Ther Targets*. 2014;18:277–292.
- Morgenstern DA, Baruchel S, Irwin MS. Current and future strategies for relapsed neuroblastoma: challenges on the road to precision therapy. *J Pediatr Hematol Oncol*. 2013;35:337–347.
- Fruci D, Cho WC, Nobili V, Locatelli F, Alisi A. Drug Transporters and Multiple Drug Resistance in Pediatric Solid Tumors. *Curr Drug Metab*. 2016;17:308–316.
- Li C, Yang C, Wei G. Vandetanib inhibits cisplatin-resistant neuroblastoma tumor growth and invasion. *Oncol Rep*. 2018;39:1757–1764.
- Piskareva O, Harvey H, Nolan J, et al. The development of cisplatin resistance in neuroblastoma is accompanied by epithelial to mesenchymal transition in vitro. *Cancer Lett*. 2015;364:142–155.
- Schlessinger A, Geier E, Fan H, et al. Structure-based discovery of prescription drugs that interact with the norepinephrine transporter, NET. *Proc Natl Acad Sci U S A*. 2011;108:15810–15815.
- Streby KA, Shah N, Ranalli MA, Kunkler A, Cripe TP. Nothing but NET: a review of norepinephrine transporter expression and efficacy of 131I-mIBG therapy. *Pediatr Blood Cancer*. 2015;62:5–11.
- Sharp SE, Trout AT, Weiss BD, Gelfand MJ. MIBG in Neuroblastoma Diagnostic Imaging and Therapy. *Radiographics*. 2016;36:258–278.
- Zhang H, Xie F, Cheng M, Peng F. Novel Meta-iodobenzylguanidine-Based Copper Thiosemicarbazide-1-guanidinomethylbenzyl Anticancer Compounds Targeting Norepinephrine Transporter in Neuroblastoma. *J Med Chem*. 2019;62:6985–6991.
- Kayano D, Kinuya S. Iodine-131 metaiodobenzylguanidine therapy for neuroblastoma: reports so far and future perspective. *Sci World J*. 2015;2015, 189135.
- Holtke C. isoDGR-Peptides for Integrin Targeting: Is the Time Up for RGD? *J Med Chem*. 2018;61:7471–7473.
- Neubauer S, Rechenmacher F, Brimiouille R, et al. Pharmacophoric modifications lead to superpotent alphavbeta3 integrin ligands with suppressed alpha5beta1 activity. *J Med Chem*. 2014;57:3410–3417.
- Desgrosellier JS, Cheresh DA. Integrins in cancer: biological implications and therapeutic opportunities. *Nat Rev Cancer*. 2010;10:9–22.
- Klim JR, Fowler AJ, Courtney AH, et al. Small-molecule-modified surfaces engage cells through the alphavbeta3 integrin. *ACS Chem Biol*. 2012;7:518–525.
- Kapp TG, Rechenmacher F, Neubauer S, et al. A Comprehensive Evaluation of the Activity and Selectivity Profile of Ligands for RGD-binding Integrins. *Sci Rep*. 2017;7: 39805.
- Mas-Moruno C, Rechenmacher F, Kessler H. Cilengitide: the first anti-angiogenic small molecule drug candidate design, synthesis and clinical evaluation. *Anticancer Agents Med Chem*. 2010;10:753–768.
- Weber WA, Haubner R, Vabulienne E, Kuhnast B, Wester HJ, Schwaiger M. Tumor angiogenesis targeting using imaging agents. *Q J Nucl Med*. 2001;45:179–182.
- Davis PJ, Davis FB, Mousa SA, Luidens MK, Lin HY. Membrane receptor for thyroid hormone: physiologic and pharmacologic implications. *Annu Rev Pharmacol Toxicol*. 2011;51:99–115.
- Davis PJ, Lin HY, Sudha T, et al. Nanotetrac targets integrin alphavbeta3 on tumor cells to disorder cell defense pathways and block angiogenesis. *Oncotargets Ther*. 2014;7:1619–1624.
- Lin HY, Mousa SA, Davis PJ. Demonstration of the Receptor Site for Thyroid Hormone on Integrin alphavbeta3. *Methods Mol Biol*. 2018;1801:61–65.
- Davis PJ, Davis FB, Lin HY, Mousa SA, Zhou M, Luidens MK. Translational implications of nongenomic actions of thyroid hormone initiated at its integrin receptor. *Am J Physiol Endocrinol Metab*. 2009;297:E1238–E1246.
- Mousa SA, Davis FB, Mohamed S, Davis PJ, Feng X. Pro-angiogenesis action of thyroid hormone and analogs in a three-dimensional in vitro microvascular endothelial sprouting model. *Int Angiol*. 2006;25:407–413.
- Mousa SA, O'Connor L, Davis FB, Davis PJ. Proangiogenesis action of the thyroid hormone analog 3,5-diiodothyropropionic acid (DITPA) is initiated at the cell surface and is integrin mediated. *Endocrinology*. 2006;147:1602–1607.
- Luidens MK, Mousa SA, Davis FB, Lin HY, Davis PJ. Thyroid hormone and angiogenesis. *Vascul Pharmacol*. 2010;52:142–145.
- Mousa SA. Compositions of dual thyrointegrin antagonists and use in vascular-associated disorders US; 2017.
- Bridoux A, Khan RA, Chen C, et al. Design, synthesis, and biological evaluation of bifunctional thyrointegrin inhibitors: new anti-angiogenesis analogs. *J Enzyme Inhib Med Chem*. 2011;26:871–882.
- Glinkskii AB, Glinksky GV, Lin HY, et al. Modification of survival pathway gene expression in human breast cancer cells by tetraiodothyroacetic acid (tetrac). *Cell Cycle*. 2009;8:3562–3570.
- Mousa SA, Bergh JJ, Dier E, et al. Tetraiodothyroacetic acid, a small molecule integrin ligand, blocks angiogenesis induced by vascular endothelial growth factor and basic fibroblast growth factor. *Angiogenesis*. 2008;11:183–190.
- Yalcin M, Dyskin E, Lansing L, et al. Tetraiodothyroacetic acid (tetrac) and nanoparticulate tetrac arrest growth of medullary carcinoma of the thyroid. *J Clin Endocrinol Metab*. 2010;95:1972–1980.
- Rajabi M, Godugu K, Sudha T, Bharali DJ, Mousa SA. Triazole Modified Tetraiodothyroacetic Acid Conjugated to Polyethylene Glycol: High Affinity Thyrointegrin alphavbeta3 Antagonist with Potent Anticancer Activities in Glioblastoma Multiforme. *Bioconjug Chem*. 2019;30:3087–3097.
- Mousa SA, Rajabi M, Karakus OO. Composition and method for dual targeting in treatment of neuroendocrine tumors, US; 2019.
- Karakus OO, Godugu K, Rajabi M, Mousa SA. Dual Targeting of Norepinephrine Transporter (NET) Function and Thyrointegrin alphavbeta3 Receptors in the Treatment of Neuroblastoma. *J Med Chem*. 2020;63:7653–7662.
- Mousa SA, Rajabi M. Non-Cleavable Polymer Conjugated with  $\alpha\beta3$  Integrin Thyroid Antagonists, US; 2019.
- Kouns WC, Kirchofer D, Hadvary P, et al. Reversible conformational changes induced in glycoprotein IIb-IIIa by a potent and selective peptidomimetic inhibitor. *Blood*. 1992;80:2539–2547.
- Wilkinson JH. Synthesis of some possible metabolites of thyroxine and triiodothyronine. *Biochem J*. 1956;63:601–605.